Plant, Cell and Environment (1997) **20,** 537–557

Simple scaling of photosynthesis from leaves to canopies without the errors of big-leaf models

D. G. G. DE PURY & G. D. FARQUHAR

Environmental Biology, Research School of Biological Sciences, Institute of Advanced Studies, The Australian National University, Canberra, ACT, Australia

ABSTRACT

In big-leaf models of canopy photosynthesis, the Rubisco activity per unit ground area is taken as the sum of activities per unit leaf area within the canopy, and electron transport capacity is similarly summed. Such models overestimate rates of photosynthesis and require empirical curvature factors in the response to irradiance. We show that, with any distribution of leaf nitrogen within the canopy (including optimal), the required curvature factors are not constant but vary with canopy leaf area index and leaf nitrogen content. We further show that the underlying reason is the difference between the time-averaged and instantaneous distributions of absorbed irradiance, caused by penetration of sunflecks and the range of leaf angles in canopies.

These errors are avoided in models that treat the canopy in terms of a number of layers – the multi-layer models. We present an alternative to the multi-layer model: by separately integrating the sunlit and shaded leaf fractions of the canopy, a single layered sun/shade model is obtained, which is as accurate and simpler. The model is a scaled version of a leaf model as distinct from an integrative approach.

Key-words: big-leaf model; modelling canopy photosynthesis; optimal distribution of leaf nitrogen.

INTRODUCTION

Models of canopy gas exchange provide a theoretical framework for thorough analysis and interpretation of the scaling of physiological processes, enabling physiologists to extend their work to larger scales. This paper aims to provide this framework, by use of a canopy model that is process-based, physically realistic, yet sufficiently simple to be effectively parametrized. Such models also fit the requirements of assessing effects of climate change on vegetation.

Photosynthesis of a canopy element depends, *inter alia*, on the biochemical capacity for photosynthesis of that element (the amount of Rubisco, ribulose-1,5-bisphosphate carboxylase/oxygenase, and electron-transport capacity), its temperature, its carbon dioxide concentration at the sites of carboxylation, and its absorbed irradiance. We first review how radiation absorption and then biochemical capacity are incorporated into models of canopy photosynthesis, and then consider recent attempts to aggregate absorbed irradiance and capacity into a single element: the so-called big-leaf model. We then present a new model that overcomes the limitations of big-leaf models and evaluate it by comparison with a multi-layer model. We also compare it with field data of canopy gas exchange.

Correspondence: David de Pury, Department of Biology, University of Antwerpen (UIA), Universiteitsplein 1, B-2610 Wilrijk, Belgium.

Absorbed irradiance

Models of canopy photosynthesis must consider the heterogeneous radiation in canopies and the non-linear response of photosynthesis to irradiance, as demonstrated by many authors (Sinclair, Murphy & Knoerr 1976; Norman 1980; Smolander 1984). Recognition that radiation attenuation through canopies can be described by Beer's law (Monsi & Saeki 1953) has led to several models of radiation penetration and absorption through canopies (Warren Wilson 1960; de Wit 1965; Ross & Nilson 1967; Cowan 1968; Ross 1975, 1981; Goudriaan 1977). It is now generally accepted that penetration of radiation through canopies must separately consider beam and diffuse radiation, due to their different attenuation in canopies, as well as visible and near-infrared wavelengths due to differential absorptance by leaves (Goudriaan 1977).

Models of radiation penetration became the basis for several comprehensive models of canopy photosynthesis (de Wit 1965; Duncan *et al*. 1967; Lemon, Stewart & Shawcroft 1971; Norman 1979), which are currently used in crop models (Whisler *et al*. 1986). They divide the canopy into multiple layers with many different leaf angle classes, for which absorbed irradiance is used to determine leaf photosynthesis. Numerical integration of photosynthesis from each leaf class yields canopy photosynthesis. The flexibility of multi-layer models allows within-canopy profiles of both environmental and physiological variables to be incorporated. While these models have been used for many applications, their complexity and the number of calculations involved with their multi-leaf-class description of canopies is a drawback for their inclusion in models of global carbon cycling (Sellers *et al*. 1992).

Radiation penetration in multi-layer photosynthesis models has been successfully simplified by considering only two classes of leaves: sunlit and shaded (Sinclair *et al*.

1976; Norman 1980). This simplification is effective because photosynthesis of shade leaves has an essentially linear response to irradiance, while photosynthesis of leaves in sunflecks is often light saturated, and independent of irradiance, allowing averaging of irradiance in each of these classes with little error in the final predicted canopy photosynthesis. However, further simplification to models with only a single leaf class can introduce large errors and lead to predictions which are inadequate for many purposes (Sinclair *et al*. 1976; Norman 1980; Boote & Loomis 1991).

Another approach to the simplification of canopy photosynthesis models is to derive analytical solutions (Acock *et al*. 1978; Johnson & Thornley 1984) and so avoid numerical integration of multi-layer models. However, analytical solutions have so far only been derived from equations of rectangular hyperbolae, for the response of leaf photosynthesis to irradiance, which do not fit measurements as well as non-rectangular hyperbolae. Predictions of canopy photosynthesis based on rectangular hyperbolae are not as close to measured rates as those from the sun/shade type models (Boote & Loomis 1991).

Biochemical capacity for photosynthesis

Within-canopy profiles of leaf nitrogen (or photosynthetic capacity) have been shown to be significantly non-uniform in canopies of a diverse range of species (wheat, Spiertz & Ellen 1978; peach, DeJong & Doyle 1985; *Solidago altissima*, Hirose & Werger 1987; *Lysimachia vulgaris*, Pons *et al*. 1989; *Carex acutiformis*, Schieving *et al*. 1992; sunflower, Sadras, Hall & Connor 1993; rice, soybean, sorghum and amaranthus, Anten, Schieving & Werger 1995). Profiles of leaf properties can be incorporated into multi-layer models of canopy photosynthesis and have a significant effect (Meister *et al*. 1987). They are also accommodated by canopy models with analytical solutions based on rectangular-hyperbolic responses to irradiance (Acock *et al*. 1978), but to date have not been easily incorporated into the simpler sun/shade models of canopy photosynthesis, except by empirical adjustments (Boote & Loomis 1991).

Profiles of leaf properties have led to the hypothesis that leaves adapt or acclimate to their radiation environment such that a plant's nitrogen resources may be distributed to maximize daily canopy photosynthesis (Field 1983; Hirose & Werger 1987). An optimal distribution of leaf nitrogen exists when any re-allocation of nitrogen would decrease daily photosynthesis. It has been further hypothesized that the optimal distribution of nitrogen occurs when the nitrogen is distributed in proportion to the distribution of absorbed irradiance in the canopy, averaged over the previous several days to a week, the time over which leaves are able to adapt. Analyses of several canopy models have supposedly supported the latter hypothesis (Hirose & Werger 1987; Wu 1993; Badeck 1995; Sands 1995). However, contrary to the earlier demonstration that separate treatment of sunlit and shaded leaves is essential in canopy models (Sinclair *et al*. 1976; Norman 1980), all these models have ignored the penetration of sunflecks and made the assumption of 100% diffuse radiation (Terashima & Hikosaka 1995). While totally diffuse radiation may be a reasonable assumption for some of the canopies examined where cloudy conditions predominate, it is unlikely to be reasonable in canopies exposed to sunny conditions and is not a reasonable assumption for models that attempt to generalize the hypothesis to all canopies.

Big-leaf models

The concept of an optimal distribution of leaf nitrogen has also been used as the basis for a new generation of big-leaf models of canopy photosynthesis (Sellers *et al*. 1992; Amthor 1994; Lloyd *et al*. 1995). It was demonstrated by Farquhar (1989) that the equation describing whole-leaf photosynthesis would have the same form as for individual chloroplasts across a leaf, provided the distribution of chloroplast photosynthetic capacity is in proportion to the profile of absorbed irradiance and that the shape of the response to irradiance is identical in all layers. This can also be extended to canopies. If the distribution of photosynthetic capacity between leaves is in proportion to the profile of absorbed irradiance then the equation describing leaf photosynthesis will also represent canopy photosynthesis (Sellers *et al*. 1992).

The big-leaf models contradict the accepted practice in modelling canopy photosynthesis whereby, at a minimum, separation into sunlit and shade leaves is considered essential for accurate predictions. The analogy of leaves in a canopy with chloroplasts in a leaf breaks down because of differences in the nature of radiation distribution in each system. In a leaf, radiation is (mostly) scattered in all directions by the first layer of cells, although its extinction through the leaf is still described by Beer's law. In a canopy, while the time-averaged profile of absorbed irradiance and the spatially averaged instantaneous profiles show an exponential decline with cumulative leaf area index (i.e. described by Beer's law), the actual instantaneous distribution of absorbed irradiance does not. Leaves in sunflecks deep in the canopy have much higher absorbed irradiance than Beer's law would predict. Additionally, irradiance in canopies is dominated by direct beam radiation (80–90% of photosynthetically active radiation, PAR, under clear skies), so that leaf angle is critical in determining the absorbed irradiance (Lambert's law). Leaves perpendicular to the sun's rays absorb maximum irradiance, while leaves parallel to the sun's rays absorb the least from only diffuse and scattered irradiance (Fig. 1). Because of the range of leaf angles some leaves, despite being at the top of the canopy, will only absorb a little irradiance. In summary, instantaneous profiles of absorbed irradiance in canopies do not follow Beer's law because of both sunfleck penetration and leaf angles. Given that the distribution of absorbed irradiance is always changing, there can be no fixed distribution of photosynthetic capacity that is proportional to absorbed irradiance (unless the

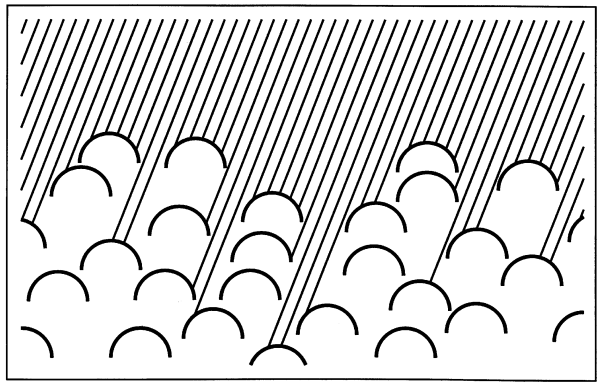

Figure 1. Radiation penetration through a canopy of uniform leaf angle distribution, which is represented by a random arrangement of hemispherical arrays of leaves. Direct beam irradiance is predominantly intercepted by leaves at the top of the canopy, but some sunflecks penetrate even to the lowest leaves. The irradiance of the leaves depends on the angle at which the beam strikes the leaf surface. Leaves perpendicular to the beam absorb the greatest amount of irradiance, but represent the least leaf area, and those parallel the least irradiance, but the greatest leaf area.

radiation is totally diffuse), so that the requirements for big-leaf models to represent accurately instantaneous canopy photosynthesis cannot be met.

Big-leaf models overcome these limitations by using an empirical coefficient to smooth the transition from irradiance-limited to irradiance-saturated canopy photosynthesis (Sellers *et al*. 1992; Amthor *et al*. 1994), or by empirical adjustment (or tuning or fitting) of canopy photosynthetic capacity or the curvature of the light response of photosynthesis (Lloyd *et al*. 1995). This reduces the overestimation of photosynthesis that would have occurred from using the averaged absorbed irradiance without adjustments. What implications does this have? Numerically, perhaps very few, since big-leaf models have been shown to describe canopy photosynthesis (Amthor *et al*. 1994; Lloyd *et al*. 1995). A problem with this type of correction is that empirical coefficients may not be independent of conditions, thus reducing the accuracy of predictions at different conditions, for example, different leaf area indices or light regimes. More fundamentally, these big-leaf models are not truly scaled models (Norman 1993; Raupach 1995), in the strict sense that the variables have different definitions and relations with one another at each scale. Thus, use of big-leaf models to scale from leaves to canopies may lead to misinterpretation of canopy dynamics in terms of the known behaviour of photosynthesis at the leaf scale.

The big-leaf model based on the relationship between the profiles of absorbed irradiance and leaf nitrogen is a potentially powerful means to reduce the complexity of models of canopy photosynthesis. This new approach needs to be reconciled with evidence from earlier work that leaves of sunlit and shaded leaves must be treated separately (Sinclair *et al*. 1976; Norman 1980). It is desirable to combine these two approaches, so that the distribution of photosynthetic resources (whether optimal or not) can be combined with the accuracy of canopy models which treat sunlit and shade leaves separately.

Outline of present approach

In this paper, we examine the effect of sunfleck penetration and leaf angles in multi-layer model predictions of the optimal distribution of canopy nitrogen. We demonstrate that the optimal distribution of canopy nitrogen is an invalid basis for the simplifications in big-leaf models. We show that big-leaf models require empirical curvature coefficients, and that these coefficients need to vary with leaf area index, the fraction of diffuse irradiance and leaf nitrogen content, or large errors result. These non-uniform distributions of canopy nitrogen (optimal or otherwise) are incorporated into a sun/shade model of canopy photosynthesis that analytically integrates the photosynthetic capacity and absorbed irradiance of the sunlit and shaded leaves separately. The new model provides predictions which are nearly as good as those of a multi-layer model, and significantly better than those of big-leaf models.

MODEL

Leaf photosynthesis

This paper addresses methods of aggregating leaf photosynthesis to canopy photosynthesis. Thus, while acknowledging the inadequacies in the modelling of leaf photosynthesis, for our purposes we assume that leaf photosynthesis is given by the model of Farquhar, von Caemmerer & Berry (1980) as described by Evans & Farquhar (1991) (and summarized with modifications in Table 1 using symbols for constants and variables defined in Tables 2 & 3). Strictly, we are assessing steady-state photosynthesis, ignoring light fluctuations at time scales smaller than a second or so where the leaves may temporally 'average' the irradiance (Kriedemann, Töröfalvy & Smart 1973).

Some of our parametrization requires comment: we have used values for Rubisco parameters based on gas exchange measurements (von Caemmerer *et al*. 1994) where the internal resistance to CO_2 diffusion from intercellular air spaces to the chloroplast is taken as zero. We have confirmed that introducing such a resistance and the changes in Rubisco parameters, in turn required to fit gas exchange data, has a < 1% effect on canopy photosynthesis (unpublished results). Similarly, we have ignored the gradual transition from electron-transport to Rubisco limitation (Kirschbaum & Farquhar 1984; Collatz *et al*. 1991) under which co-limitation occurs, since this too has little effect on canopy photosynthesis, as only a small fraction of leaves are near the transition to light saturation at any moment.

Leaf respiration that continues in the light, R_l, is assumed to scale with Rubisco capacity, in that the value at 25 °C is taken as $0{\cdot}0089V_l$. This is equivalent to assuming a fixed CO_2 compensation point, Γ (Eqn 7), of 4·4 Pa at 25 °C, which is a reasonable value for wheat (Watanabe, Evans & Chow

Table 1. Equations of the Farquhar *et al*. (1980) leaf photosynthesis model. Symbols are defined in Tables 2 and 3. Values of the Rubisco parameters are given in Table 4

Equation	Definition	No.
$A_l = \min\{A_j, A_v\} - R_l$	Net rate of leaf photosynthesis	(1)
$A_v = V_l \dfrac{p_i - \Gamma_*}{p_i + K'}$, providing $p_i > \Gamma_*$	Rubisco-limited photosynthesis	(2)
$K' = K_c (1 + O/K_o)$	Effective Michaelis-Menten constant	(3)
$A_j = J \dfrac{p_i - \Gamma_*}{4(p_i + 2\Gamma_*)}$, providing $p_i > \Gamma_*$	Electron-transport limited rate of photosynthesis	(4)
$\theta_l J^2 - (I_{le} + J_m) J + I_{le} J_m = 0$	Irradiance dependence of electron transport	(5)
$I_{le} = I_l (1 - f)/2$	PAR effectively absorbed by PSII	(6)
$\dfrac{R_l}{V_l} = \dfrac{\Gamma - \Gamma_*}{\Gamma + K'}$	Ratio of leaf respiration to photosynthetic Rubisco capacity	(7)
$k_T = k_{25} \exp(E_a(T - 25)/[298\, R(T + 273)])$	Arrhenius function	(8)
$\Gamma_* = 3{\cdot}69 + 0.188(T - 25) + 0{\cdot}0036(T - 25)^2$	Temperature dependence of Γ_*	(9)
$J_{m_T} = J_{m_{25}} \cdot \exp\left[\dfrac{(T_K - 298)E_a}{RT_K \cdot 298}\right] \dfrac{\left[1 + \exp\left(\dfrac{S \cdot 298 - H}{R \cdot 298}\right)\right]}{\left[1 + \exp\left(\dfrac{ST_K - H}{RT_K}\right)\right]}$	Temperature (K) dependence of J_m	(10)

1994). The variation of R_l with temperature is assumed to independently follow an Arrhenius form (Eqn 8 & Table 4).

Temperature dependences of other model parameters have also been modelled by the Arrhenius function; the activation energies are presented in Table 4. Many plants acclimate to the growth temperature regime so that the temperature dependence of membrane-bound processes, such as electron transport, change with growth temperature (Björkman, Badger & Armond 1980; Sayed, Earnshaw & Emes 1989). Expressions to describe temperature acclimation may need to include this phenomenon, which is ignored here.

We have assumed a fixed ratio of $J_m/V_l = 2{\cdot}1$ at 25 °C (Wullschleger 1993), although the ratio does vary with temperature in proportion to the ratio of the temperature sensitivities of the components (Fig. 2).

Canopy photosynthesis

In uniform crop canopies, the main source of variation in the physical environment is irradiance. Since the response of photosynthesis to irradiance is non-linear (Eqns 4 & 5) the method of spatial integration can introduce errors; for example, use of irradiance averaged over the whole canopy causes an overestimation of photosynthesis (Smolander 1984). The requirement for accuracy at this level of detail needs to be weighed against the complexity of the model and the concomitant increase in the number of calculations required (Norman 1980).

The problem of integrating the non-linear response of leaf photosynthesis to irradiance can be overcome by the use of multi-layer models, which rely on numerical integration. We first describe a multi-layer model that is used for subsequent comparisons with simpler canopy models.

Multi-layer integration

This method of calculating canopy photosynthesis is based on the radiation penetration modelling by Goudriaan (1977) as summarized in Appendix 1 and the CUPID model (Norman 1982). The canopy was split into multiple layers (increments in L of 0·1). Each layer was separated into sunlit and shaded fractions (Eqn A1 in Table A1 of Appendix 1) and the sunlit fraction divided into nine leaf angle classes (Eqn A9). Absorbed irradiance was calculated for the shaded fraction (Eqn A7) and for each leaf class of the sunlit fractions (Eqn A12) separately.

Table 2. Table of constants used in all the canopy photosynthesis models

Symbol	Value	Units	Description (constants at 25°C)
Irradiance model constants			
f_a	0·426	–	forward scattering coefficient of PAR in atmosphere
k_d	0·78	–	diffuse PAR extinction coefficient
L_e	147°20·5' E	degrees	local longitude (Wagga Wagga, Australia)
L_s	150° E	degrees	standard longitude of time zone
P	$98{\cdot}7\times10^3$	Pa	atmospheric air pressure
P_o	$101{\cdot}3\times10^3$	Pa	atmospheric air pressure at sea level
λ	–35°3·5' S	degrees	latitude (Wagga Wagga, Australia)
ρ_{cd}	0·036	–	canopy reflection coefficient for diffuse PAR
ρ_h	0·04	–	reflection coefficient of a canopy with horizontal leaves
ρ_l	0·10	–	leaf reflection coefficient for PAR
τ_l	0·05	–	leaf transmissivity to PAR
σ	0·15	–	leaf scattering coefficient of PAR ($\rho_l + \tau_l$)
Photosynthesis model constants			
E_a	(see Table 4)	J mol^{-1}	activation energy
f	0·15	–	spectral correction factor
H	220000	J mol^{-1}	curvature parameter of $J_{m_{(T)}}$
K_c	40·4	Pa	Michaelis-Menten constant of Rubisco for CO_2
K_o	$24{\cdot}8\times10^3$	Pa	Michaelis-Menten constant of Rubisco for O_2
K'	73·8	Pa	Effective Michaelis-Menten constant of Rubisco
O	$20{\cdot}5\times10^3$	Pa	oxygen partial pressure
R	8·314	J mol^{-1} K^{-1}	Universal gas constant
S	710	J K^{-1} mol^{-1}	electron-transport temperature response parameter
Γ	4·4	Pa	CO_2 compensation point of photosynthesis
Γ_*	3·69	Pa	Γ in the absence of mitochondrial respiration
θ_l	0·7	–	curvature of leaf response of electron transport to irradiance

Table 3. List of variables, categorized by the models in which they are used

Symbol	Units	Description (constants at 25°C)
Temporary variables used in model development		
I_e	μmol m^{-2} s^{-1}	extra-terrestrial PAR
N_d	μmol m^{-2} sr^{-1}	diffuse photon radiance of the sky, Id(0)/2π
α	radians	angle of beam irradiance to the leaf normal
Irradiance model variables common to all models		
a	–	atmospheric transmission coefficient of PAR
f_d	–	fraction of diffuse irradiance
h	radians	hour angle of the sun, $\pi(t-t_o)/12$
k_b	–	beam radiation extinction coefficient of canopy, 0·5/sinβ
k'_b	–	beam and scattered beam PAR extinction coefficient, 0·46/sinβ
k'_d	–	diffuse and scattered diffuse PAR extinction coefficient, 0·719
L_c	m^2 m^{-2}	canopy leaf-area index
m	–	optical air mass, (P/P_o)/sinβ
t	h	time of day
t_o	h	time of solar noon
t_d	d	time since beginning of year
β	radians	solar elevation angle
δ	radians	solar declination angle
ρ_{cb}	–	canopy reflection coefficient for beam PAR
Photosynthesis model variables common to all models		
A_c	μmol m^{-2} s^{-1}	rate of canopy photosynthesis per unit ground area
A_j	μmol m^{-2} s^{-1}	rate of photosynthesis limited by RuBP regeneration
A_v	μmol m^{-2} s^{-1}	rate of photosynthesis limited by Rubisco

Table 3. Continued

Symbol	Units	Description (constants at 25°C)
I_{le}	μmol m^{-2} s^{-1}	PAR effectively absorbed by PSII per unit leaf area
J	μmol m^{-2} s^{-1}	rate of electron transport rate per unit leaf area
J_m	μmol m^{-2} s^{-1}	potential rate of electron transport rate per unit leaf area
k_n	–	coefficient of leaf-nitrogen allocation in a canopy
N_b	mmol m^{-2}	leaf nitrogen not associated with photosynthesis
N_l	mmol m^{-2}	leaf nitrogen concentration per unit leaf area
N_o	mmol m^{-2}	leaf nitrogen concentration at top of canopy
p_i	Pa	intercellular CO_2 partial pressure
R_c	μmol m^{-2} s^{-1}	canopy respiration per unit ground area
T	°C	leaf temperature
V_l	μmol m^{-2} s^{-1}	photosynthetic Rubisco capacity per unit leaf area
χ_n	mmol mol^{-1} s^{-1}	ratio of photosynthetic capacity to leaf nitrogen
Specific to the big-leaf model (per unit ground area)		
I_c	μmol m^{-2} s^{-1}	PAR absorbed by the canopy
N_c	mmol m^{-2}	total canopy leaf nitrogen content
V_c	μmol m^{-2} s^{-1}	photosynthetic Rubisco capacity of canopy
θ_c	–	curvature factor of response of canopy photosynthesis to irradiance
Specific to the Sun/Shade model (per unit ground area)		
f_{cSun}	–	fraction of canopy that is sunlit
I_{cSh}	μmol m^{-2} s^{-1}	PAR absorbed by the shaded fraction of the canopy
I_{cSun}	μmol m^{-2} s^{-1}	PAR absorbed by the sunlit fraction of the canopy
V_{cSh}	μmol m^{-2} s^{-1}	photosynthetic Rubisco capacity of shaded fraction of canopy
V_{cSun}	μmol m^{-2} s^{-1}	photosynthetic Rubisco capacity of sunlit fraction of canopy
Specific to the multi-layer model		
$A_l(L)$	μmol m^{-2} s^{-1}	rate of leaf photosynthesis per unit leaf area
$f_{1,2}(L)$	–	fraction of leaf area in a leaf-angle class
$f_{Sh}(L)$	–	fraction of leaves that are shaded
$f_{Sun}(L)$	–	fraction of leaves that are sunlit
$g(\alpha_l)$	–	distribution function of leaf-area orientation
$I_b(L)$	μmol m^{-2} s^{-1}	beam PAR per unit ground area
$I_d(L)$	μmol m^{-2} s^{-1}	diffuse PAR per unit ground area
$I_l(L)$	μmol m^{-2} s^{-1}	total absorbed PAR per unit leaf area
$I_{lbb}(L)$	μmol m^{-2} s^{-1}	absorbed beam PAR without scattering per unit leaf area
$I_{lbs}(L)$	μmol m^{-2} s^{-1}	absorbed scattered beam PAR per unit leaf area
$I_{lb}(L)$	μmol m^{-2} s^{-1}	absorbed beam plus scattered beam PAR per unit leaf area
$I_{ld}(L)$	μmol m^{-2} s^{-1}	absorbed diffuse plus scattered diffuse PAR per unit leaf area
$I_{lbSun}(L)$	μmol m^{-2} s^{-1}	beam PAR absorbed by sunlit leaves per unit leaf area
$I_{lSh}(L)$	μmol m^{-2} s^{-1}	total PAR absorbed by shaded leaves per unit leaf area
I_{lSun}	μmol m^{-2} s^{-1}	total PAR absorbed by sunlit leaves per unit leaf area
L	m^2 m^{-2}	cumulative leaf-area index from top of canopy ($L = 0$ at top)
$R_l(L)$	μmol m^{-2} s^{-1}	leaf respiration per unit leaf area
$V_l(L)$	μmol m^{-2} s^{-1}	catalytic capacity of Rubisco per unit leaf area
α_l	radians	angle of beam irradiance to the leaf normal

Distribution of leaf nitrogen, N_l, between leaves in the canopy was modelled as decreasing exponentially with cumulative relative leaf area index, L/L_c, from the top of the canopy (Hirose & Werger 1987), modified to reflect the distribution of nitrogen associated with photosynthesis and a base level of leaf nitrogen, N_b, not associated with photosynthesis (Anten *et al*. 1995). The distribution of leaf nitrogen in the canopy is not necessarily related to the profile of absorbed irradiance. Leaf nitrogen distribution, $N_l(L)$, in the canopy was described relative to a nominal leaf nitrogen content at the top of the canopy, N_o, according to the equation

$$N_l = (N_o - N_b)\exp(-k_n L/L_c) + N_b, \quad (11)$$

where k_n is the coefficient of leaf nitrogen allocation and L_c is the canopy leaf area index.

Leaf nitrogen was converted to Rubisco capacity, V_l, assuming a linear relationship between V_l and N_l (Evans 1983; Field & Mooney 1986) with a residual leaf nitrogen content of N_b = 25 mmol m^{-2} (i.e. ≈0·5% N, when $V_l = 0$),

$$V_l = \chi_n (N_l - N_b), \quad (12)$$

where χ_n is the ratio of measured Rubisco capacity to leaf

Table 4. Photosynthesis parameters at 25 °C and their activation energies, E_a (kJ mol^{-1}). The Rubisco parameters K_c, K_o and Γ_* are appropriate to an infinite internal conductance to CO_2 diffusion

Parameter	Value	E_a
K_c (Pa)	[a]40·4	[b]59 400
K_o (Pa)	[a]$24{\cdot}8\times10^3$	[b]36 000
V_l (μmol m^{-2} s^{-1})	~	[b]64 800
J_m (μmol m^{-2} s^{-1})	[e]$2{\cdot}1V_l$	[c]37 000
R_l (μmol m^{-2} s^{-1})	[e]$0{\cdot}0089V_l$ (@ 25 °C)	[c]66 400
Γ_* (Pa)	[a]3·69	[d]29 000

[a]von Caemmerer *et al*. (1994); [b]Badger & Collatz (1977); [c]Farquhar *et al*. (1980); [d]Jordan & Ogren (1984); [e]Watanabe *et al*. (1994).

N. χ_n was calculated from values of V_l (from leaf photosynthesis measurements) and from measurements of N_l.

Leaf nitrogen was calculated for leaves of each layer (Eqn 11) and converted to photosynthetic capacity (Eqn 12). Leaf photosynthesis was calculated for each leaf class (Eqns 1–6) less leaf respiration calculated from the Rubisco capacity (Table 4). Canopy photosynthesis rate was calculated by the summation of the product of rate of leaf photosynthesis per unit leaf area by the leaf area in each class (Eqn A9).

Distribution of leaf nitrogen and absorbed irradiance

Measurements of incident radiation were used in the multi-layer model to generate the predicted distribution of absorbed irradiance in relation to the distribution of leaf nitrogen in the canopy (Fig. 3). Model parameters were obtained from measurements in a canopy of wheat (Table 5) or from published values (Table 4). A *spatially averaged instantaneous* profile of absorbed irradiance was calculated by averaging the absorbed irradiance of all leaves (sunlit and shaded) in a layer at midday (maximum solar elevation was 68° above the horizon). Integration of all such distributions for all times during the day gave the *daily* profile of absorbed irradiance (Fig. 3).

An assumption in the big-leaf model is that leaf nitrogen should be distributed in a canopy in proportion to the profile of absorbed irradiance. It can be seen in Fig. 3 that this wheat canopy did have a distribution of leaf nitrogen that was approximately in proportion to the profile of *daily* absorbed irradiance. If leaf nitrogen were exactly distributed in proportion to the absorbed irradiance, the modelled distribution would have been a straight line across the figure extrapolating to zero irradiance at N = 25 mmol m^{-2}. In addition, an *instantaneous* profile of *spatially averaged* absorbed irradiance is also shown in Fig. 3. This too has a distribution that is nearly in proportion to the profile of leaf nitrogen.

With the parameters for the multi-layer model set as above, an *instantaneous* distribution of absorbed irradiance in relation to leaf nitrogen content was predicted for the sunlit and shaded leaves separately with leaf angles from a uniform leaf angle distribution (Fig. 4). The distribution presented was calculated for midday; other times gave similar distributions but at lower levels of absorbed irradiance. The vertical (or z) axis indicates the relative distribution of leaves at each level of absorbed irradiance for the sunlit leaves and the absolute distribution of the shaded leaves (the distribution of sunlit leaves is shown on a relative scale because the absolute distribution depends on the number of leaf angle classes). A uniform leaf angle distribution was assumed (i.e. all orientations are equally represented; also known as a spherical distribution), so that the probability, $g(\alpha_l)$, of a leaf being at an angle between α_l and $\alpha_l + d\alpha_l$ is $\Pr(\alpha_l, \alpha_l + d\alpha_l) = \sin\alpha_l\, d\alpha_l$. This leaf angle distribution function together with the fraction of sunlit leaf

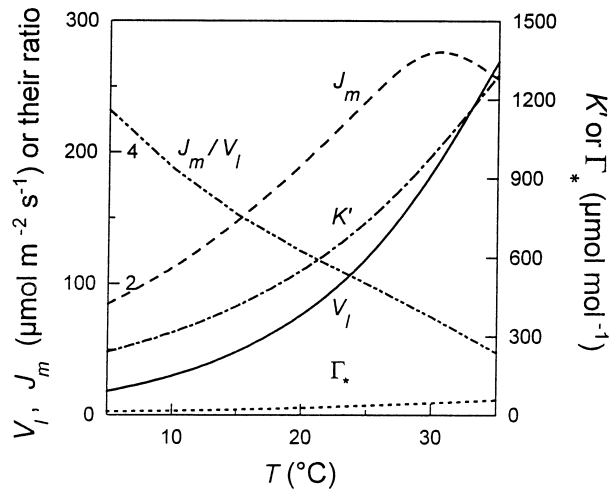

Figure 2. Effect of temperature on leaf photosynthesis parameters: *Left axis* (outside labels): V_l (μmol m^{-2} s^{-1}), J_m (μmol m^{-2} s^{-1}); (inside labels) the ratio J_m/V_l. *Right axis*: K' (Eqn 3, μmol mol^{-1} CO_2) and Γ_* (μmol mol^{-1} CO_2) modelled using activation energies in Table 4.

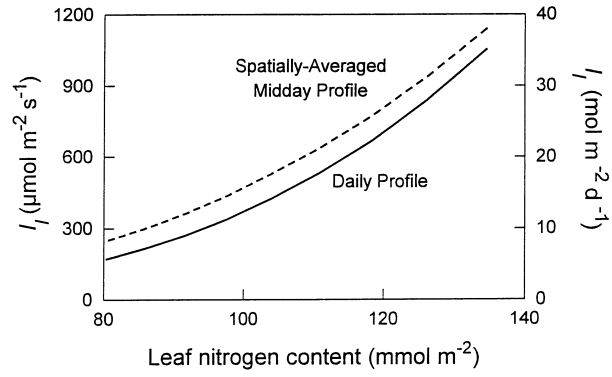

Figure 3. Modelled distribution of the midday spatially averaged (for sunlit and shaded leaves) (– – –, μmol m^{-2} s^{-1}) and daily average (— —, mol m^{-2} d^{-1}) absorbed irradiance (quanta) per unit leaf area by leaves in a homogenous canopy, of uniform leaf angle distribution, as a function of the observed leaf nitrogen content (mmol m^{-2}).

Table 5. Model parameter values (per unit leaf area) obtained from leaf measurements in a wheat crop, cultivar Matong, at Wagga Wagga, NSW, 4 d after anthesis

Parameter	Value	Units
Date	25 Oct (day 298)	–
latitude	–35° 3·5' S	degrees
a	0.72	–
L_c	2.4	$m^2\ m^{-2}$
V_l	110	$\mu mol\ m^{-2}\ s^{-1}$
N_l	120	$mmol\ m^{-2}$
N_o	137	$mmol\ m^{-2}$
k_n	0.713	–

area (Eqn A1) generated the curved surface and is shown as the relative proportion of sunlit leaves on the left-hand vertical or z axis [$\Pr(\alpha_l, \alpha_l + d\alpha_l)/d\alpha_l = \sin\alpha_l$]. Each layer of the canopy, as indicated by leaf nitrogen content, has a range of absorbed irradiance for the sunlit leaves at different leaf angles (calculated from Eqn A12). Leaves nearly perpendicular to the sun-beam direction have the highest absorbed irradiance (1830–2040 $\mu mol\ m^{-2}\ s^{-1}$), and are only a small proportion of the sunlit leaves, while leaves parallel to the beam direction absorbed only diffuse radiation (220–430 $\mu mol\ m^{-2}\ s^{-1}$) and are a high proportion of the sunlit leaves. This distribution of irradiance may be visualized if, for example, one imagines the sun shining directly at the north pole: the intensity would be greatest at the pole and least at the equator, and the surface area of the earth in a latitudinal band (say of 10°) would be least at the pole and greatest at the equator. At any particular leaf angle, absorbed irradiance decreases slightly with depth in the canopy due to the attenuation of diffuse and scattered radiation.

The proportion of sunlit leaves decreased with each successive layer deeper in the canopy (indicated by lower leaf nitrogen). The proportion of each layer shaded increased with depth in the canopy, shown as the vertical plane at the rear of Fig. 4 and the right-hand or z axis.

In contrast to the distribution of *spatially averaged* absorbed irradiance, the relationship between absorbed irradiance and leaf nitrogen is very different when the sunlit and shaded fractions of the canopy are shown *separately* (Fig. 4). No longer is the instantaneous distribution of absorbed irradiance even approximately in proportion to the distribution of leaf nitrogen (i.e. a diagonal line). The profile of leaf nitrogen and the distribution of absorbed irradiance for the sunlit and shaded leaves of the canopy show no semblance of being proportional to each other.

Inspection of the *average* irradiance profiles (Fig. 3) suggests that leaf nitrogen was approximately distributed in proportion to profiles of both daily and *spatially averaged* instantaneous absorbed irradiance. However, if the distribution of instantaneous absorbed irradiance of sunlit and shade leaves is used, then it is apparent that the distribution of leaf nitrogen is not in proportion to the profile of absorbed irradiance (Fig. 4) and therefore the basis for the simplifications in the big-leaf model is not valid.

This conflict arises because the *time-averaged* and *spatially averaged* distributions of absorbed irradiance in a canopy are quite different from the *instantaneous* distribution of absorbed irradiance, when sunfleck penetration and the effect of leaf angles are considered. As stated in the introduction, canopy modellers have long recognized the importance of treating sunlit and shaded leaves separately (Sinclair *et al*. 1976; Norman 1980). The analysis presented here has applied that principle to the profiles of absorbed irradiance and leaf nitrogen, as assumed in the new generation of big-leaf models (Sellers *et al*. 1992; Amthor 1994; Lloyd *et al*. 1995). If profiles of average irradiance are used, contradicting the practice of keeping sunlit and shaded leaves separate, then the profile of absorbed irradiance can mistakenly be shown to be in proportion to the profile of leaf nitrogen. A big-leaf model working from this assumption will then have errors associated with averaging the irradiance profiles, which have been shown to be large (Sinclair *et al*. 1976; Norman 1980). In the models of Sellers *et al*. (1992) and Amthor (1994) the errors are not apparent because of the introduction of a curvature factor in the response of canopy photosynthesis to absorbed irradiance. We will demonstrate the effect of this curvature factor later.

Optimal distribution of leaf nitrogen

Profiles of *spatially averaged* absorbed irradiance are also used in several models that examine the optimal distribu-

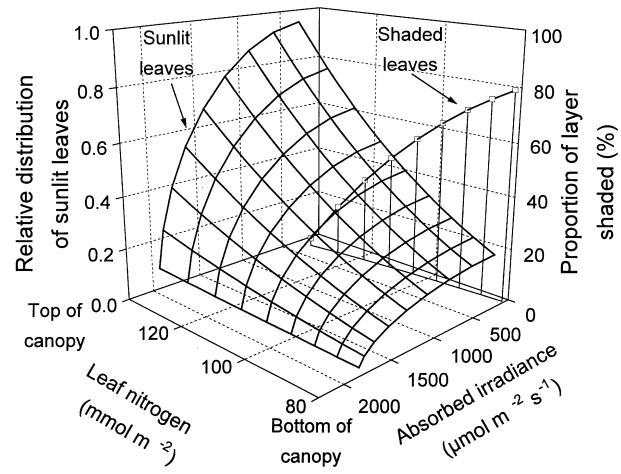

Figure 4. Model predictions of the instantaneous distribution of absorbed irradiance (quanta) per unit leaf area for sunlit and shaded leaves ($\mu mol\ m^{-2}\ s^{-1}$) in relation to the leaf nitrogen distribution. Profiles were generated as in Fig. 3. The vertical axis on the left is the relative probability distribution of sunlit leaves with respect to absorbed irradiance defined by the leaf angle, and is $\Pr(\alpha_l, \alpha_l + d\alpha_l)/d\alpha_l = \sin\alpha_l$. The relative distribution of sunlit leaves is represented by the three-dimensional surface (left vertical axis). The distribution of irradiance on shaded leaves was assumed independent of leaf angle and is represented by the vertical plane at the lowest absorbed irradiance levels (–□– , right vertical axis). See text for further details.

tion of leaf nitrogen to maximize canopy photosynthesis (Hirose & Werger 1987; Wu 1993; Badeck 1995; Sands 1995). They use this approach as it greatly simplifies the analysis, but, unless the canopies are grown under continuous diffuse radiation, the profile of spatially averaged irradiance will not be a realistic representation of canopies receiving direct-beam radiation, which have sunflecks penetrating to all levels of the canopy and (assuming a uniform leaf angle distribution) with a range of leaf angles with different amounts of absorbed irradiance at all levels in the canopy.

To demonstrate the effect of using the spatially averaged irradiance, we parametrized the multi-layer model as described above, but with canopy layers of increment in L of 0·5 and five leaf angle classes (to speed the optimization) and examined the distribution of leaf nitrogen required to maximize the daily integral of canopy photosynthesis. Total canopy photosynthetic Rubisco capacity per unit ground area was kept constant at 224 μmol m^{-2} s^{-1}, but reallocated between different layers. Two approaches were taken regarding assumptions about absorbed irradiance in calculations of leaf photosynthesis. In the first, the irradiance was averaged from all leaves of a layer to calculate the average rate of photosynthesis. In the second, absorbed irradiance for each of the five leaf angle classes of sunlit and shaded leaves was calculated separately and converted to leaf photosynthesis. The profile of average absorbed irradiance was, of course, identical in both cases. The distribution of leaf photosynthetic capacity to maximize canopy photosynthesis over a day was determined for each case by calculating the sensitivity of photosynthesis of each layer to an additional unit of photosynthetic capacity, dA/dV. Units of photosynthetic capacity were manually moved from layers with low values of dA/dV to layers with high values of dA/dV, until all layers had equal values of dA/dV, which is the condition of maximum canopy photosynthesis (Field 1983). This manual redistribution of photosynthetic capacity avoided any assumptions about the shape of the resultant distributions of leaf photosynthetic capacity in the canopy. The distributions that generated the maximum canopy photosynthesis under both assumptions are shown together with the actual measured distribution in Fig. 5.

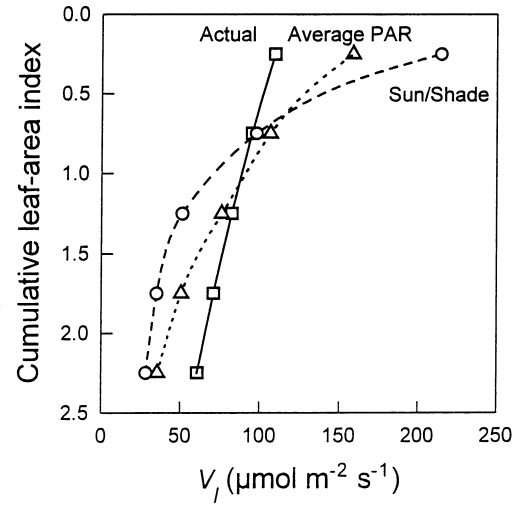

Figure 5. Modelled distributions of leaf photosynthetic capacity, based on measurements in a wheat canopy (Actual, –□–) and the profiles required to maximize canopy photosynthesis using spatially averaged absorbed irradiance for each layer (Average PAR, ···△···) or using calculations for sunlit and shaded leaves separately (sun/shade, – – ○ – –).

The actual profile of leaf photosynthetic capacity (measured in the field and described by parameters in Table 5) was significantly different from a uniform distribution of leaf photosynthetic capacity. Both apparent optimal distributions had steeper profiles of leaf photosynthetic capacity than the measured profile, with a higher capacity at the top and less capacity lower in the canopy. The true optimal distribution obtained with calculations based on separate sunlit and shaded leaves was steeper than when the light was averaged. In contrast, Terashima & Hikosaka (1995) supposed that if sunfleck penetration was considered then the optimal distribution of canopy nitrogen would be less steep than if totally diffuse radiation was assumed, because sunflecks would deliver more radiation deeper into the canopy. However, in the modelling presented here, the profile of absorbed irradiance was identical in both cases. The only difference was the separation into sunlit and shaded leaves. The distribution of canopy nitrogen required to maximize canopy photosynthesis under totally diffuse radiation (data not shown) was very similar to the distribution required to maximize canopy photosynthesis based on the average irradiance described above.

Maximum daily canopy photosynthesis based on separate sunlit and shaded leaves increased by 9% compared to that obtained with the actual nitrogen distribution, but increased by only 5% when based on the average irradiance. Daily canopy photosynthesis with the actual distribution of leaf photosynthetic capacity was 19% greater when calculations were based on average irradiance compared to that calculated with separate sunlit and shaded leaves. Clearly, assumptions about averaging of irradiance in a canopy affect conclusions as to the optimal distribution of leaf photosynthetic capacity.

The above calculations were made assuming a linear relationship between photosynthetic capacity and leaf nitrogen content which may in fact be better represented by a non-linear relationship. This may change the resultant distributions of leaf nitrogen required to maximize photosynthesis, but would not alter the fact that ignoring sunflecks and assuming an average irradiance results in a different optimal distribution of leaf nitrogen compared to the distribution obtained by consideration of sunflecks. The truly optimal distribution of leaf nitrogen is more strongly influenced by the time leaves spend in sunflecks rather than by the distribution of absorbed irradiance *per se*. This is because the sensitivity of Rubisco-limited photosynthesis (PAR saturated) to nitrogen, dA_v/dN, is much greater than the sensitivity of electron-transport-limited photosynthesis, dA_j/dN.

Big-leaf model

As outlined in the Introduction, the parallel profiles of leaf photosynthetic capacity and absorbed irradiance suggest an alternative approach to canopy integration: scaling by use of a big-leaf model. This assumes that the canopy can be represented by a single layer having capacity for photosynthesis and a single irradiance. This assumption is valid when the vertical profile of photosynthetic capacity is optimally distributed to maximize photosynthesis, which in turn means that it is distributed in proportion to the absorbed irradiance profile (Farquhar 1989). While the distribution of photosynthetic capacity in a canopy may be optimal for maximizing *daily* photosynthesis, it cannot be simultaneously optimal for maximizing *instantaneous* photosynthesis at all *instants* of time, since leaf photosynthetic capacity cannot be reallocated between leaves on the time scale of irradiance variation in a canopy. Irradiance distribution in a canopy varies as radiation penetration changes with the traverse of the sun across the sky on its diurnal and seasonal course. By contrast, photosynthetic capacity can only be redistributed in a canopy over a period of several days in response to changes in the daily average irradiance profile, but cannot adjust on the time scale of seconds and minutes associated with the movement of sunflecks. Earlier work (Sellers *et al*. 1992; Amthor 1994; Lloyd *et al*. 1995) assumed that, because leaf nitrogen is approximately distributed in the canopy in proportion to the *time-averaged* profile of absorbed irradiance, a big-leaf model can be used to predict *instantaneous* canopy photosynthesis, but ignored the quite different nature of the *instantaneous* distribution of absorbed irradiance due to penetration of sunflecks and the effect of leaf angles on absorbed irradiance.

To illustrate the problems that result even when a curvature factor is introduced, we present a big-leaf model which integrates the input profiles and calculates a single photosynthetic rate as though the canopy were a single big leaf. Canopy absorbed irradiance, nitrogen, photosynthetic capacity and leaf respiration were calculated for the entire canopy by integration as outlined below. The leaf photosynthesis model (Eqns 1–6) was then applied to the canopy as though it were a single big leaf.

Absorbed irradiance of canopies

Irradiance absorbed by a canopy, per unit ground area, was determined by integrating I_l (Eqn A6) over the entire canopy leaf area (L_c = m^2 leaf m^{-2} ground):

$$\begin{aligned} I_c &= \int_0^{L_c} I_l dL \\ &= (1-\rho_{cb})\, I_b(0)[1-\exp(-k_b' L_c)] \\ &\quad +(1-\rho_{cd}) I_d(0)[1-\exp(-k_d' L_c)]. \end{aligned} \tag{13}$$

Canopy nitrogen and photosynthetic capacity

Total canopy nitrogen, N_c, was calculated by integration of the leaf nitrogen profile (Eqn 11) over the entire canopy:

$$\begin{aligned} N_c &= \int_0^{L_c} N_l dL \\ &= L_c\{(N_o - N_b)[1-\exp(-k_n)]/k_n + N_b\}. \end{aligned} \tag{14}$$

Canopy photosynthetic capacity, V_c, was calculated as the integral of leaf photosynthetic capacity over the entire canopy:

$$\begin{aligned} V_c &= \int_0^{L_c} V_l dL = \chi_n \int_0^{L_c} (N_l - N_b)\, dL \\ &= L_c \chi_n (N_o - N_b)[1-\exp(-k_n)]/k_n. \end{aligned} \tag{15}$$

Leaf respiration of the canopy, R_c, was calculated by integration of leaf respiration:

$$\begin{aligned} R_c &= \int_0^{L_c} R_l dL \\ &= V_c R_l / V_l, \end{aligned} \tag{16}$$

where R_l/V_l is the ratio of leaf respiration to leaf Rubisco capacity at 25 °C (Eqn 7). Canopy photosynthesis is then calculated by using I_c and V_c in the leaf photosynthesis model (Eqns 1–10).

An improvement in the performance of big-leaf models occurs when a process analogous to the co-limitation of photosynthesis by both electron transport and Rubisco at the leaf level (Kirschbaum & Farquhar 1984; Collatz *et al*. 1991) is applied to canopies (Sellers *et al*. 1992; Wang & Jarvis 1993; Amthor 1994). Mathematically this is achieved by a non-rectangular hyperbola,

$$\theta_c A_c^2 - (A_j + A_v) A_c + A_j A_v = 0, \tag{17}$$

where A_c is determined as the smaller root of the solution. The curvature of the response of canopy photosynthesis to irradiance is principally determined by the value of θ_c, and to a lesser extent θ_l (Eqn 5). Note that the models of Collatz *et al*. (1991), Sellers *et al*. (1992) and Amthor (1994) have no curvature, θ_l, in the relationship between A_j and I_{le}, but this has little bearing on the present treatment.

Comparison of big-leaf and multi-layer models

Predictions from several multi-layer models have been compared with field measurements of canopy photosynthesis and were capable of adequately reproducing diurnal trends (Lemon *et al*. 1971; Caldwell *et al*. 1986; Norman & Polley 1989; Grant 1992). Tuned big-leaf models (i.e. with fitted values of θ_c) are also capable of reproducing observed trends. The issue here, however, is the extent to which simplifications can be made to multi-layer models while still preserving the correspondence between leaf properties and canopy performance. Multi-layer models have traditionally been used as a baseline for comparing simplified canopy integration schemes (Sinclair *et al*. 1976; Norman 1980; 1993; Goudriaan 1986; Johnson, Parsons & Ludlow 1989; Reynolds *et al*. 1992; Baldocchi 1993). Such comparisons between models allow structural

differences to be tested without the compounding effects of parameter uncertainties and are again used here.

The predicted response of canopy photosynthesis to absorbed irradiance was compared for the multi-layer and big-leaf canopy models (Fig. 6). (The simulations were conducted at a constant leaf temperature of 20 °C and p_i = 27·0 Pa.) The diurnal variation of incident irradiance was taken from measurements at Wagga Wagga, Australia, on 25 October (de Pury 1995) with a simulated diurnal variation of the fraction of diffuse irradiance as determined by the solar path length through the atmosphere (Eqn A25). Simulations for the big-leaf model were made by adjusting the canopy curvature factor, θ_c, to obtain the best fit with the multi-layer model under typical clear sky radiation (f_d = 0·15 at solar noon, θ_c = 0·877). The same value of θ_c was used at high leaf area index. Canopy nitrogen was, implicitly, scaled with the leaf area index as defined by the exponential nitrogen profile based on relative leaf area index (Eqns 11 and 14). An alternative assumption would be to describe the nitrogen profile as a function of the absolute leaf area index [i.e. $N = N_o \exp(-k_i L)$] (as would happen, for example, if nitrogen were to remain in proportion to the daily irradiance profile as a canopy grows). Simulations by the multi-layer model were used as the standard for evaluation of the big-leaf model.

Despite tuning, the big-leaf model predictions did not closely match the response of canopy photosynthesis to absorbed irradiance predicted by the multi-layer model, overestimating by up to 14% at intermediate irradiances and then underestimating at higher irradiances.

At high leaf area index, the big-leaf model (with θ_c = 0·877 fitted at low leaf area index) overestimated canopy photosynthesis by up to 50% at some instants (Fig. 6). Better simulations by the big-leaf model were obtained by again adjusting the curvature factor, though the response to irradiance still did not match the multi-layer model.

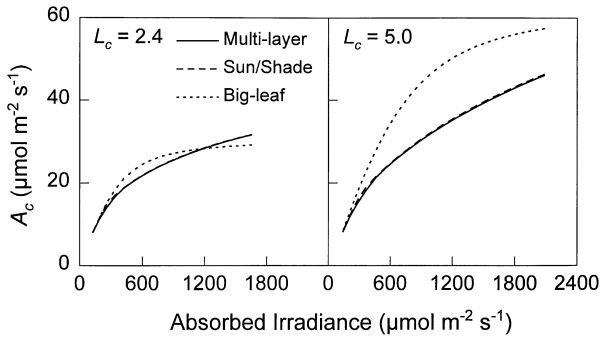

Figure 6. Comparison of simulated response of canopy photosynthesis to absorbed irradiance for the multi-layer (— —), sun/shade (– – –) and big-leaf (·····) models at different leaf area indices, L_c = 2·4 (*left*) and L_c = 5·0 (*right*) under clear sky conditions (a = 0·75, Eqn A25). Simulations from the big-leaf model are shown with θ_c = 0·877, obtained by fitting under clear sky. The same value of θ_c was used for the simulations at high leaf area index. Note that the sun/shade model predictions coincide with and are obscured by the multi-layer model predictions.

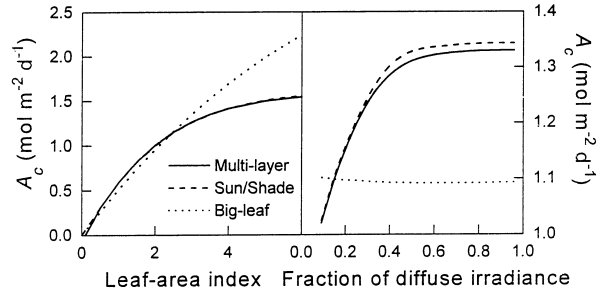

Figure 7. Effect of varying leaf area index, L_c (*left*), and fraction of diffuse irradiance, f_d (*right*), on daily canopy photosynthesis predicted by the multi-layer (— —) , sun/shade (– – –) and big-leaf (·····) models. Model simulations were made using diurnal irradiance data on 25 October with coefficients obtained from a wheat crop, cultivar Matong (de Pury 1995) (Table 5) and a fitted θ_c = 0·877. Canopy nitrogen content was implicitly scaled with leaf area index by Eqns 11 and 14. Variation in the fraction of diffuse radiation was generated by varying the atmospheric transmission coefficient (Eqn A25).

Similar discrepancies in the irradiance response of the big-leaf model were found with alternative nitrogen distributions.

The models were further analysed by comparing predictions of daily canopy photosynthesis over a range of leaf area indices and fractions of diffuse irradiance (Fig. 7). The fraction of diffuse irradiance, f_d, was varied by changing the atmospheric transmission coefficient (Eqn A25), but with constant total irradiance. Model predictions of daily canopy photosynthesis are shown as a function of the minimum value of f_d at solar noon (Fig. 7).

The predictions of the big-leaf model were 20% higher than those of the multi-layer model at a leaf area of 4 and 45% higher at a leaf area index of 6 (Fig. 7). In contrast, when the nitrogen distribution was proportional to the daily irradiance profile, the big leaf model predictions of daily canopy photosynthesis improved significantly (errors ranging from –10% to +4% with increasing leaf area index). The performance of the big leaf model was strongly affected by the leaf nitrogen allocation in the canopy and its dynamics with changing leaf area index. The big-leaf model was relatively unresponsive to f_d, while in contrast the multi-layer model demonstrated a 30% increase in daily photosynthesis in changing from very clear sky to totally diffuse radiation. When leaf photosynthetic capacity was changed, the big-leaf model again overestimated canopy photosynthesis by up to 10% (data not shown). There was no effect of CO_2 concentration on the performance of the big-leaf model (data not shown).

Selection of a value of θ_c in the big-leaf model is difficult *a priori*, but easier *a posteriori*. We fitted the big-leaf model by adjusting the value of θ_c such that the big-leaf model predictions matched the multi-layer model predictions by minimizing the sum of residuals squared. The value of θ_c, required to give the best fit, varied with the leaf area index, the distribution of leaf nitrogen, the leaf-nitro-

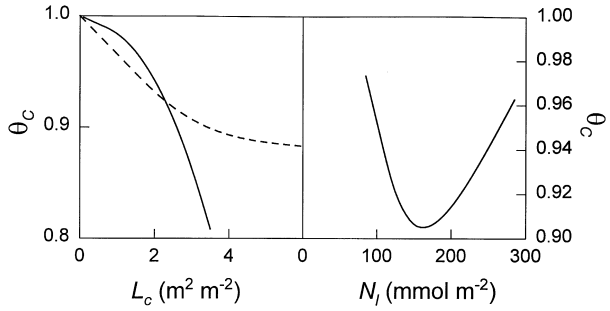

Figure 8. Variation of the co-limitation parameter of canopy photosynthesis, θ_c, with canopy leaf area index assuming canopy nitrogen distribution is described by Eqn 14 (——) or if N is proportional to daily irradiance profile (– – –) (*left*) and with leaf nitrogen content of leaves at the top of the canopy (*right*). Values were obtained from fitting the big-leaf model predictions to those of the multi-layer model and minimizing the sum of residuals squared. Simulations were made with the same conditions as in Fig. 7.

gen content (Fig. 8) and fraction of diffuse radiation, but not with atmospheric CO_2 concentration.

Use of curvature factors in canopy-photosynthesis models is attractive since it allows the use of simple big-leaf models. Unfortunately, the value of θ_c is not constant, but varies with canopy leaf area index, fraction of diffuse irradiance, leaf-nitrogen content and its distribution in the canopy.

An alternative approach, still using the big-leaf model but without θ_c, is to empirically reduce canopy photosynthetic capacity. With a 30% reduction, predictions of daily canopy photosynthesis by the big-leaf model were then equivalent to those from the multi-layer model, but this did not improve the shape of the response of canopy photosynthesis to absorbed irradiance. Empirical corrections to big-leaf models have been proposed previously (Johnson *et al.* 1989), and were similar to those found here, but again their selection *a priori* is difficult.

Sun/shade model

The penetration of beam irradiance, its variation through the day and the range of leaf angles in a canopy of uniform leaf angle distribution all affect the ability of a big-leaf model to simulate the diurnal changes in canopy photosynthesis. These canopy features can be explicitly incorporated by dividing the canopy into sunlit and shaded fractions and modelling each fraction separately with a single-layer model. We call this the sun/shade model. It is more complex than a big-leaf model, but its more detailed treatment of the irradiance profiles overcomes some of the errors associated with the simplifying assumptions of a big-leaf model. We include variation of photosynthetic capacity with depth, and use the currently accepted biochemical model of leaf photosynthesis in this new synthesis.

This new approach splits the big-leaf model into sunlit and shaded fractions. Since these fractions change during the day with solar elevation (changing k_b in Eqn A1), so too the irradiance absorption and the photosynthetic capacity of sunlit and shaded leaf fractions change. Photosynthetic capacities of individual leaves do not change during the day, but the division between the sunlit and shaded portions of the canopy does. Calculation of irradiance absorption and photosynthetic capacity of the separate sunlit and shaded fractions is outlined in the following sections.

Absorbed irradiance of sunlit and shaded fractions of canopies

Irradiance absorbed by the sunlit leaf fraction of the canopy (I_{cSun}) is calculated as an integral of absorbed irradiance (Eqn A12) and the sunlit leaf area fraction (Eqn A1). This irradiance is absorbed by only the sunlit part of the canopy. Although not explicitly used in this model, the sunlit leaf area index of the canopy is

$$L_{Sun} = \int_0^{L_c} f_{Sun}(L)\,dL = [1-\exp(-k_b L_c)]/k_b, \qquad (18)$$

while the shaded leaf area index of the canopy is $L_{Sh} = L_c - L_{Sun}$, which can be used to calculate the average irradiance and photosynthetic capacity of the sunlit and shaded fractions from the fraction totals given below.

Irradiance absorbed by the separate sunlit and shade fractions of the canopy is defined such that the total irradiance absorbed (I_c, Eqn 13) is the sum of the two parts,

$$I_c = I_{cSun} + I_{cSh}. \qquad (19)$$

The total irradiance absorbed by the canopy and the components absorbed by the sunlit and shaded fractions are all expressed on a ground-area basis. The irradiance absorbed by the sunlit fraction of the canopy is given as the sum of direct-beam, diffuse and scattered-beam components

$$\begin{aligned} I_{cSun} &= \int_0^{L_c} I_{lSun}(L) f_{Sun}(L)\,dL \\ &= \int_0^{L_c} I_{lb}(L) f_{Sun}(L)\,dL + \int_0^{L_c} I_{ld}(L) f_{Sun}(L)\,dL \\ &\quad + \int_0^{L_c} I_{lbs}(L) f_{Sun}(L)\,dL, \end{aligned} \qquad (20a)$$

which are, for direct-beam irradiance absorbed by sunlit leaves, using Eqns A2 and A1,

$$\int_0^{L_c} I_{lb}(L) f_{Sun}(L)\,dL = I_b(0)(1-\sigma)[1-\exp(-k_b L_c)] \qquad (20b)$$

(note the use of σ for sunlit leaves compared to ρ_{cb} in Eqn A2 for the average of all leaves); for diffuse irradiance absorbed by sunlit leaves, using Eqns A5 and A1,

$$\begin{aligned} \int_0^{L_c} I_{ld}(L) f_{Sun}(L)\,dL &= I_d(0)(1-\rho_{cd}) \\ &\quad \times \{1-\exp[-(k'_d+k_b)L_c]\}k'_d/(k'_d+k_b), \end{aligned} \qquad (20c)$$

and for scattered-beam irradiance absorbed by sunlit leaves, using Eqns A8 and A1,

$$\int_0^{L_c} I_{lbs}(L) f_{Sun}(L)\,dL$$
$$= I_b(0)\begin{bmatrix}(1-\rho_{cb})\{1-\exp[-(k'_b+k_b)L_c]\}k'_b/(k'_b+k_b)\\ -(1-\sigma)[1-\exp(-2k_bL_c)]/2\end{bmatrix}. \quad (20d)$$

Irradiance absorbed by the shaded leaf area of the canopy is given by an integral of absorbed irradiance in the shade (Eqn A7) and the shaded leaf area fraction ($f_{Sh} = 1 - f_{Sun}$), shown in Appendix 2. More simply, it is calculated as the difference between the total irradiance absorbed by the canopy, I_c (Eqn 13), and the irradiance absorbed by the sunlit leaf area, I_{cSun} (Eqn 20a):

$$I_{cSh} = I_c - I_{cSun}. \quad (21)$$

An example of canopy absorption of irradiance and its separation into sunlit and shaded fractions is presented in Fig. 9.

Photosynthetic capacity of sunlit and shaded leaf fractions

The diurnal progress of the sun traversing the sky results in continual movement of sunflecks in a canopy. When the sun is low in the sky, direct beam radiation is mostly intercepted by leaves at the top of the canopy. Conversely, when the sun is high in the sky, sunflecks penetrate deeper into the canopy. The partitioning of leaves into sunlit and shaded fractions is continually changing throughout the day. Calculation of the photosynthetic capacity of these separate fractions needs to reflect these dynamics. That is not to say that the photosynthetic capacity of individual leaves is continually being adjusted, but rather that the division of the leaves into sunlit or shaded fractions is changing.

Photosynthetic capacity of the sunlit leaf-fraction of the canopy, V_{cSun}, was calculated by integrating the leaf photosynthetic capacity (Eqn 12) and the sunlit leaf area fraction (Eqn A1):

$$V_{cSun} = \int_0^{L_c} V_l(L) f_{Sun}(L)\,dL$$
$$= L_c \chi_n (N_o - N_b)[1-\exp(-k_n - k_bL_c)]/(k_n + k_bL_c). \quad (22)$$

Photosynthetic capacity of the shaded leaf fraction of the canopy, V_{cSh}, may be calculated by an integral of the leaf photosynthetic capacity (Eqn 12) and the shaded leaf area fraction (also from Eqn A1), shown in Appendix 2. As with the calculation of absorbed irradiance, V_{cSh} can be more simply calculated as the difference between canopy photosynthetic capacity (Eqn 15) and the photosynthetic capacity of the sunlit fraction (Eqn 22):

$$V_{cSh} = V_c - V_{cSun}. \quad (23)$$

An example of the distribution of photosynthetic capacity between sunlit and shaded leaf fractions of the canopy is shown in Fig. 10.

Photosynthesis of the sunlit and shaded fractions of the canopy is then calculated by use of the leaf photosynthesis model (Eqns 1–10), with the absorbed irradiance and photosynthetic capacity of each fraction, respectively, used in place of the equivalent leaf variables. Canopy photosynthesis is obtained by adding the photosynthetic contribution from the two components, minus the leaf respiration of the canopy, R_c (Eqn 16):

$$A_c = A_{cSun} + A_{cSh} - R_c. \quad (24)$$

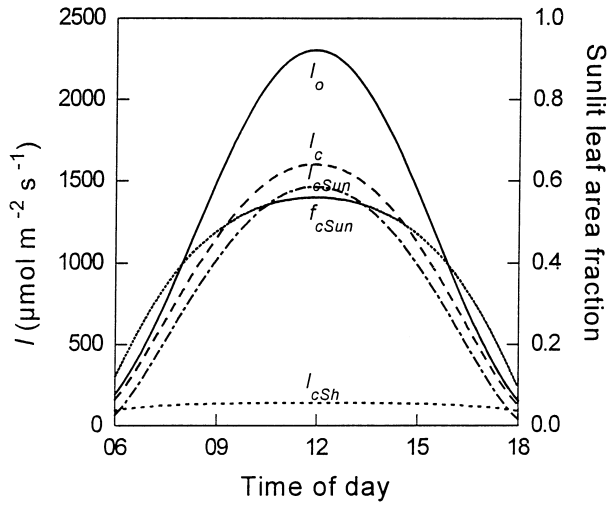

Figure 9. Modelled irradiance and absorption (per unit ground area) by a canopy of leaf area index = 2·4. I_o, total irradiance above canopy; I_c, irradiance absorbed by entire canopy; I_{cSh}, irradiance absorbed by shaded leaf fraction of canopy; I_{cSun}, irradiance absorbed by sunlit leaf fraction of canopy; f_{cSun}, sunlit leaf area fraction.

Calculation procedure

Implementation of the sun/shade model of canopy photosynthesis is demonstrated by a worked example as explained below and summarized in Table 6. Solar declination is calculated in Appendix 1 ('Solar geometry') for the particular latitude of the location and the day of the year by Eqn A14. For each time step through the day, solar elevation is calculated by Eqn A13 ($\sin\beta$ = 0·87), the canopy reflection coefficient for beam PAR by Eqn A19 (= 0·029), the canopy extinction coefficient for beam PAR by Eqn A4 (= 0·46/0·87), the fraction of sunlit leaves by Eqn A1 (= exp [–(0·5/0·87) 2·4]), and the fraction of diffuse irradiance for a cloudless sky by Eqn A25 (= 0·15), which in the conditions defined in Table 5 gives the results shown in Table 6. For the example in Table 6, incident light is given as 2083 μmol m^{-2} s^{-1}, so that diffuse and beam irradiance were calculated as $0{\cdot}159 \times 2083 = 331$ and $(1 - 0{\cdot}159) \times 2083 = 1752$ μmol m^{-2} s^{-1}, respectively. The absorbed irradiance is calculated for the sunlit leaf fraction using Eqn 20 (a, b, c & d):

$$\begin{aligned} I_{cSun} = {} & 1752(1-0{\cdot}15)\{1-\exp[-(0{\cdot}5/0{\cdot}87)2{\cdot}4]\} \\ & + 331(1-0{\cdot}036)\{1-\exp[-(0{\cdot}719+0{\cdot}5/0{\cdot}87)2{\cdot}4]\} \\ & \times 0{\cdot}719/(0{\cdot}719+0{\cdot}5/0{\cdot}87) \\ & + 1752\begin{bmatrix}(1-0{\cdot}029)\{1-\exp[-(0{\cdot}46/0{\cdot}87+0{\cdot}5/0{\cdot}87)\\ 2{\cdot}4]\}(0{\cdot}46/0{\cdot}87)/(0{\cdot}46/0{\cdot}87+0{\cdot}5/0{\cdot}87)\\ -(1-0{\cdot}15)\{1-\exp[-2(0{\cdot}5/0{\cdot}87)2{\cdot}4]\}/2\end{bmatrix} \\ = {} & 1116+170+61=1347, \end{aligned}$$

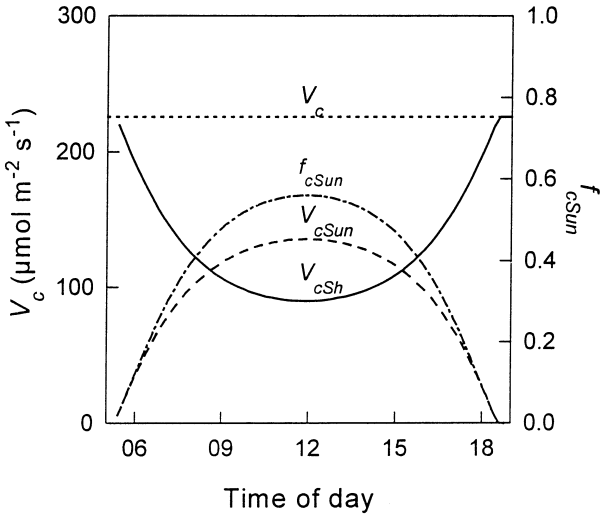

Figure 10. Photosynthetic capacity of the entire canopy, V_c, (Eqn 15) and separated into sunlit, V_{cSun} (Eqn 22), and shaded, V_{cSh} (Eqn 23), leaf fractions. The fraction of the canopy that is sunlit, f_{cSun}, is also shown. Corrections for diurnal variation of temperature are not shown.

and for the shaded leaf fraction from Eqns 13 and 20a:

$$I_{cSh} = 1752(1-0{\cdot}029)\{1-\exp[-(0{\cdot}46/0{\cdot}87)2{\cdot}4]\} + 331(1-0{\cdot}036)[1-\exp(-0{\cdot}719\times 2{\cdot}4)] - I_{cSun} = 1226+263-1347 = 142.$$

Photosynthetic Rubisco capacity of the sunlit fraction of the canopy is calculated from Eqn 22 (the ratio χ_n was calculated from measured leaf photosynthetic capacity and leaf nitrogen content, Table 5 and Eqn 12; χ_n = 110/(120 – 25) = 1·16):

$$V_{cSun} = 2{\cdot}4\times 1{\cdot}16(137-25)\{1-\exp[-0{\cdot}713-(0{\cdot}5/0{\cdot}87)2{\cdot}4]\}/[0{\cdot}713+2{\cdot}4(0{\cdot}5/0{\cdot}87)] = 133$$

and photosynthetic Rubisco capacity of the shaded leaf fraction from Eqns 15 and 22:

$$V_{cSh} = 2{\cdot}4\times 1{\cdot}16(137-25)[1-\exp(-0{\cdot}713)]/0{\cdot}713 - V_{cSun} = 224-133 = 91,$$

allowing calculation of the electron-transport capacity for each fraction with the fixed ratio of J_m/V_l = 2·1 at 25 °C. Parameters of the photosynthesis model are adjusted for the effect of temperature by the Arrhenius function (Tables 1 & 4) and Eqn 10 for electron transport. The Rubisco-limited rate of photosynthesis is then calculated for the sunlit and shaded fractions of the canopy by Eqn 2, using the intercellular CO_2 concentration, which in this example is prescribed (24·5 Pa), but would usually be calculated by coupling this model with a stomatal model, an expression for the diffusion of CO_2 through stomata and boundary layers and an energy balance (de Pury 1995). The RuBP regeneration-limited rate of photosynthesis is calculated separately for the sunlit and shaded leaf fractions, by Eqns 4–6. The actual rate of photosynthesis, for either fraction, is taken as the minimum of the Rubisco-limited or RuBP regeneration-limited rate (Eqn 1). The rates of photosynthesis from the sunlit and shaded fractions are simply added to obtain total canopy photosynthesis from which canopy respiration (Eqn 16) is subtracted (Eqn 24), as shown in Table 6.

Comparison of sun/shade and multi-layer models

The simpler sun/shade model accurately reproduced the response of canopy photosynthesis to absorbed irradiance

Table 6. Calculated example of implementing the sun/shade canopy photosynthesis model, shown for 10:30h on 25 October with parameters obtained from a wheat canopy presented in Table 5 and other constants as defined in Table 2. The sunlit leaf area was 55% of the leaf-area index. All fluxes are in units of μmol m^{-2} ground s^{-1}

		Total Canopy	Sunlit Fraction	Shaded Fraction
Sine solar elevation angle	$\sin\beta$	0·87		
Canopy reflection coefficient	ρ_{cb}	0·029		
Fraction of diffuse PAR	f_d	0·159		
Intercellular CO_2 partial pressure	p_i	24·5		
Canopy temperature	T	21		
Total incident PAR	I	2083		
Absorbed irradiance	I_{cSun}, I_{cSh}		1347	142
Photosynthetic Rubisco capacity @ 25°C	V_{cSun}, V_{cSh}		133	91
Photosynthetic Rubisco capacity @ T	V_{cSun}, V_{cSh}		97	66
Electron-transport capacity @ T	J_m		234	159
Rubisco-limited photosynthesis	A_v		25·1	17·1
RuBP regeneration limited photosynthesis	A_j		36·1	9·4
Gross photosynthesis	A_{cSun}, A_{cSh}		25·1	9·4
Canopy leaf respiration	R_c	1·5		
Canopy photosynthesis		33·0		

predicted by the multi-layer model (Fig. 6, where the two responses are virtually indistinguishable). At twice the leaf area index, the sun/shade model again accurately reproduced the response of canopy photosynthesis to absorbed irradiance. Similarly, the sun/shade model was able closely to match the multi-layer model when the fraction of diffuse irradiance was varied (Fig. 7). In contrast to the big-leaf model, the predictions from the sun/shade model matched those of the multi-layer model without the use of an empirical fitting parameter.

Measured diurnal courses of environmental variables were used to predict gross canopy photosynthesis for the same wheat canopy as described previously for the 25 October. Predictions from the sun/shade model closely matched those from the multi-layer model, as shown in the previous simulations, and also matched gross canopy photosynthesis (measured net canopy CO_2 flux plus respiration) (Fig. 11). The electron-transport-limited and Rubisco-limited rates of canopy photosynthesis are shown for the sunlit and shaded fractions of the canopy as predicted by the sun/shade model. In the sun/shade model the rates of photosynthesis for the sunlit and shaded fractions of the canopy are calculated as the minimum of either the electron-transport-limited or Rubisco-limited rates. It is apparent in Fig. 11 that the shaded fraction of the canopy is always electron-transport-limited (i.e. $A_{jSh} < A_{vSh}$) and that the sunlit leaves are usually Rubisco-limited ($A_{vSun} < A_{jSun}$), except when the absorbed irradiance is very low. The fraction of leaves in the sunlit fraction increased from 0% at low irradiance to 56% at the maximum solar elevation.

Small discrepancies between the sun/shade model and the multi-layer model occurred near the point at which the sunlit fraction changed from electron-transport-limited to Rubisco-limited photosynthesis. At this irradiance, representation of photosynthesis by the sunlit fraction as limited either by electron transport or by Rubisco involves a simple averaging of a continuum of irradiance intensities caused by a range of leaf angles. As irradiance increases, the proportion of leaves in the sunlit leaf fraction that are not Rubisco-limited decreases and so this simplification improves until the errors associated with averaging are not detectable. These errors have the same source as those associated with the simplifications in the big-leaf model representation of canopy photosynthesis, but have much less impact on the accuracy of the sun/shade model than they do on the big-leaf model.

The irradiance at which the greatest discrepancy occurs is the irradiance saturation point of leaf photosynthesis (I_{lsat}), since there is no further increase in photosynthesis with increasing irradiance. It can be calculated by combining Eqns 2–6 and rearranging to yield the expression

$$I_{lsat} = V_l \frac{2}{(1-f)} \cdot \frac{4(p_i + 2\Gamma_*)[4\theta_l(p_i + 2\Gamma_*) - (J_m/V_l)(p_i + K')]}{(p_i + K')[4(p_i + 2\Gamma_*) - (J_m/V_l)(p_i + K')]} \cdot (25)$$

Several of the parameters in the calculation of the irradiance saturation point of photosynthesis are affected by temperature. Providing the ratio of J_m/V_l remains constant (at 25 °C), the irradiance saturation point is a linear function of Rubisco capacity, and the dependence on V_l increases with increasing p_i and with temperature (Fig. 12).

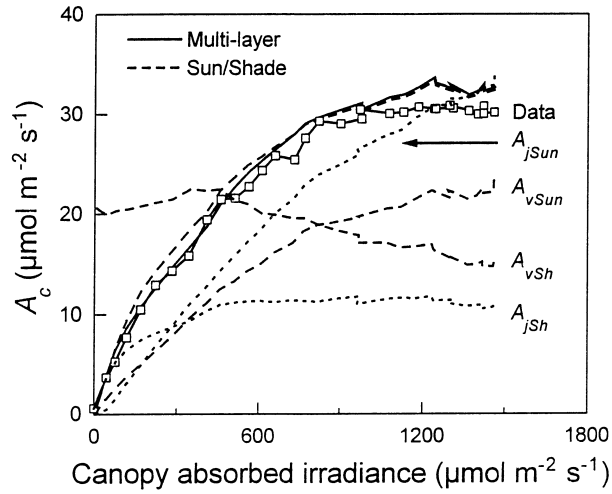

Figure 11. Response of gross canopy photosynthesis to irradiance (A_c) data (–□–) compared with predictions from the sun/shade model (– – –) and multi-layer (— —) model of canopy photosynthesis. Modelled electron-transport-limited (A_j, – – –) and Rubisco-limited (A_v, ·····) rates of photosynthesis are shown for the sunlit and shaded fractions of the canopy. Data are for a canopy of wheat, cultivar Matong, on 25 October measured by a large ventilated chamber (de Pury 1995).

CONCLUSIONS

Models of canopy photosynthesis

The sun/shade model of canopy photosynthesis presented here contains five features none of which are new individually, but are new in combination. They are (1) separate treatments of sun and shade leaves; (2) variation of photosynthetic capacity through the canopy; (3) use of current biochemical modelling of photosynthesis; (4) dynamic partitioning between sun and shade components, and (5) a single-layer model with simple computations. Perhaps the most important feature of this model is its scaling nature, so that parameters of the leaf photosynthesis model are scaled to the canopy with equivalent definitions and relationships between them at both the leaf and canopy scales.

The sun/shade model presented here is an improvement over previous sun/shade models (Sinclair *et al*. 1976; Norman 1980), as more realistic non-uniform vertical profiles of photosynthetic capacity are now incorporated into the model. The dynamic partitioning of photosynthetic capacity and irradiance between sunlit and shaded leaves has further reduced the errors associated with simplification to just a single layer in models of canopy photosynthesis (cf. Sinclair *et al*. 1976; Norman 1980; Reynolds *et al*. 1992).

The sun/shade model presented here gives predictions of canopy photosynthesis that closely match simulations from a multi-layer model, but with far fewer calculations. The

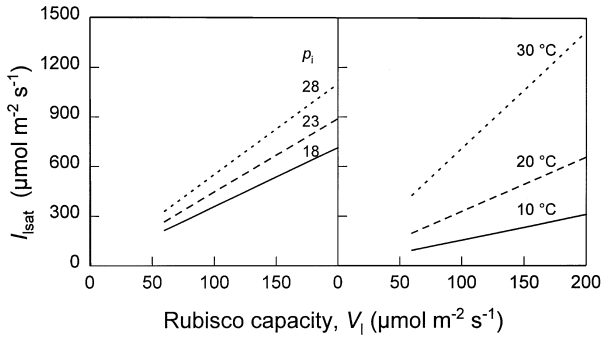

Figure 12. PAR saturation point of leaf photosynthesis (I_{lsat}) (Eqn 25), under conditions experienced in a canopy, where p_i is assumed constant while photosynthetic Rubisco capacity and irradiance decrease with depth in the canopy. The ratio of electron transport to Rubisco capacity (J_m/V_l) is assumed constant (at 25 °C). Three constant values of p_i are shown (left panel): 18 (solid line), 23 (dashed line) and 28Pa (dotted line) at 25 °C and three temperatures (right panel): 10 (solid line), 20 (dashed line) and 30 °C (dotted line) at 23Pa.

model is robust over a range of canopy leaf area indices and environmental variables. Differences between predictions of the sun/shade model, the multi-layer model and flux measurements are well within the errors of any canopy flux measurement technique and within the accuracy of parameter determination given the stochastic nature of leaf photosynthetic capacity and other parameters. The sun/shade canopy model requires only four additional equations, beyond those required in the model of leaf photosynthesis, to calculate the absorbed irradiance and photosynthetic capacity of the sunlit and shaded leaves, Eqns 20, 21, 22 and 23, respectively, which are used to calculate canopy photosynthesis. This simplicity should make it attractive for incorporation into models of crop growth, global carbon cycling and other higher-level processes.

Big-leaf models, similar to those proposed by Sellers *et al*. (1992), Amthor (1994) and Lloyd *et al*. (1995), were found to be less accurate than the sun/shade model. Approximations, implicit in the big-leaf model, were found to cause distortions in the modelled response of canopy photosynthesis to irradiance compared with the multi-layer model. There is no distribution of nitrogen or capacity that allows the big-leaf model to work directly. Fitting the canopy curvature factor in the big-leaf model did not correct all the discrepancies. The value of the curvature factor required to reproduce the response of canopy photosynthesis to irradiance, as modelled by the multi-layer model, was found to vary with canopy leaf area index, the fraction of diffuse irradiance and, to a lesser extent, leaf nitrogen content. Errors associated with using a fixed value of the curvature factor (fitted at $L_c = 2{\cdot}4$) were 20% of daily gross canopy photosynthesis at $L_c = 4$ and even greater at higher leaf area indices. For many purposes (e.g. constant L_c and constant N) these errors may not be important. However, they may be significant when the fraction of diffuse irradiance varies diurnally and with partly cloudy conditions or when canopy leaf area index is varying, such as in crop-growth models or models that predict the response of vegetation to climate change.

The big-leaf models are based on the assumption of an optimal distribution of photosynthetic capacity within the canopy in relation to the distribution of absorbed irradiance. In this study, the distribution of photosynthetic capacity did approximately follow the distribution of daily absorbed irradiance (Fig. 3) as has been observed in many other canopies (Hirose & Werger 1987; Anten *et al*. 1995). However, even a perfect match of capacity with this distribution does not validate big-leaf models. We have shown that big-leaf models are based on an incorrect assumption of the similarity of the instantaneous and time-averaged profiles of absorbed irradiance in canopies. Therefore, use of big-leaf models to analyse canopy fluxes in terms of parameters derived from leaf-scale equivalents or from the behaviour of the leaf-scale model is misleading because the parameters fitted at the canopy scale will not necessarily correspond with those at the leaf scale.

Errors involved with averaging of irradiance over sunlit and shaded leaves for use in the non-linear response of photosynthesis to irradiance are large (Sinclair *et al*. 1976; Norman 1980; Smolander 1984). The sun/shade model of canopy photosynthesis presented here overcomes these problems of big-leaf models without the need to fit the model and has the advantages of allowing within-canopy profiles of leaf photosynthetic capacity and the use of a biochemically based model of photosynthesis.

Optimal distribution of leaf nitrogen

Models that use *averaged* irradiance in canopy layers to determine the optimal distribution of photosynthetic capacity to maximize canopy photosynthesis are flawed in their implicit assumptions that the *time-averaged* and the *spatially averaged* irradiance profiles are identical to the *instantaneous* profiles of absorbed irradiance. Leaf nitrogen is, indeed, often distributed such that it follows the profile of time-averaged absorbed irradiance, but it does not mean that it also resembles the instantaneous profile of absorbed irradiance. The flawed logic results in misleading conclusions about the optimal distribution of leaf nitrogen required to maximize canopy photosynthesis.

APPENDIX 1: MULTI-LAYER MODEL OF IRRADIANCE PENETRATION IN CANOPIES

The canopy was assumed to be homogeneous with respect to the horizontal distribution of leaves with a uniform leaf angle distribution. This allows simplification of the irradiance penetration model because the distribution of the beam-leaf incidence angles is independent of solar position.

Penetration of diffuse, beam and scattered irradiance were modelled as separate components by Beer's law (Goudriaan 1977) as summarized in Table A1. k_b is the extinction coefficient of beam irradiance ($= 0{\cdot}5/\sin\beta$, for a uniform leaf angle distribution, the factor 0·5 being the

ratio of projected area to surface area of a hemisphere and β being the solar elevation) and L is the cumulative leaf area index from the top of the canopy (zero at the top). Irradiance absorbed by sunlit leaves, I_{lSun}, and that absorbed by shaded leaves, I_{lSh}, are calculated separately by assuming that diffuse, scattered diffuse and scattered beam irradiance impinges on all leaves, while sunlit leaves in addition receive direct-beam irradiance.

Absorbed irradiance of sunlit leaves

Irradiance absorbed by sunlit leaves is calculated as absorbed beam plus absorbed diffuse and absorbed scattered beam. However, while diffuse radiation and scattered radiation are assumed to be isotropic, beam radiation is unidirectional and thus the angle of incidence on leaves must be considered.

The distribution of leaf angles affects the penetration of radiation through a canopy and the angle of incidence of irradiance on leaf laminae (used to calculate the absorbed irradiance per unit leaf area by Lambert's cosine law). Absorbed irradiance is, in turn, used to calculate photosynthesis. In a multi-layer model, canopy photosynthesis is obtained by numerical integration of the leaf photosynthesis equations from all leaves. Thus, to apply Lambert's law, each layer of the canopy is divided into a number of discrete leaf angle classes (depending on the detail required). For a particular layer, the fraction of leaf area in the class between α_{l1} and α_{l2} ($f_{l1,2}$) is obtained from the integral of the leaf angle distribution function, which, in the case of a uniform leaf angle distribution, is given by Eqn A9 (Ross 1975, 1981). A mean cosine of leaf angle ($\overline{\cos\alpha_l}$) for each class is determined (Eqn A10) as this is used to calculate absorbed irradiance, rather than the cosine of the mean leaf angle ($\cos\bar{\alpha}_l$) as has been used previously (i.e. Norman 1980; Forseth & Norman 1993) [e.g. in a single leaf angle class of a uniform leaf angle distribution $\arccos(\overline{\cos\alpha_l}) = 60{\cdot}0°$ compared with $\arccos(\cos\bar{\alpha}_l) = 57{\cdot}1°$].

Absorbed irradiance calculated as $\partial I_b(L)/\partial L$ (Eqn A2) applies only to leaves at the mean cosine of the leaf angle and is the spatial average over all leaves, both sunlit and shaded. Since with a uniform leaf angle distribution all orientations are equally probable, the distribution of beam-

Table A1. Equations for radiation absorption in a multi-layer model. Symbols are defined in Table 3

Equations	Definition	No.
$f_{Sun}(L) = \exp(-k_b L)$	sunfleck penetration	(A1)
$I_{lb}(L) = (1-\rho_{cb})\, k_b I_b(0) \exp(-k_b L)$	beam irradiance — without scattering, average for all leaves	(A2)
$I_{lb}(L) = (1-\rho_{cb})\, k_b' I_b(0) \exp(-k_b' L)$	beam irradiance — with scattering, average for all leaves	(A3)
$k' = k(1-\sigma)^{1/2}$	modified extinction coefficients to account for scattering by leaves	(A4)
$I_{ld}(L) = (1-\rho_{cd})\, k_d' I_d(0) \exp(-k_d' L)$	diffuse irradiance	(A5)
$I_l = I_{lb}(L) + I_{ld}(L)$	total irradiance	(A6)
$I_{lSh}(L) = I_{ld}(L) + I_{lbs}(L)$	irradiance absorbed by shaded leaves	(A7)
$I_{lbs}(L) = I_b(0)\left[\begin{array}{l}(1-p_{cb})\, k_b' \exp(-k_b' L) \\ -(1-\sigma)\, k_b \exp(-k_b L)\end{array}\right]$	scattered beam irradiance	(A8)
$f_{l_{1,2}}(\alpha_l) = \int_{a_{l_1}}^{\alpha_{l_2}} \sin\alpha_l\, d\alpha_l = \cos\alpha_{l_1} - \cos\alpha_{l_2}$	fraction of leaves in each leaf-angle class	(A9)
$\overline{\cos\alpha_{l_{1,2}}} = \frac{1}{2}\left(\sin^2\alpha_l\right)_{\alpha_{l_1}}^{\alpha_{l_2}} \Big/ f_{l_{1,2}}(\alpha_l) = \frac{1}{2}\left(\cos\alpha_{l_1} + \cos\alpha_{l_2}\right)$	mean leaf angle of each leaf-angle class	(A10)
$I_{lbSun}(\beta) = (1-\sigma) I_b(0)\, \overline{\cos\alpha_l}/\sin\beta$	beam irradiance absorbed by sunlit leaves	(A11)
$I_{lSun}(L,\beta) = I_{lbSun}(\beta) + I_{lSh}(L)$	total irradiance absorbed by sunlit leaves	(A12)

leaf incidence angles is independent of solar position and is identical to the distribution of leaf angles. In subsequent equations, α_l represents both the angle of elevation of leaves and the angle between direct-beam irradiance and the leaf normal. However, beam intensity and the fraction of sunlit leaves are not independent of solar elevation.

Beam intensity on a plane perpendicular to the beam direction is calculated by dividing beam intensity on a horizontal plane by the sine of solar elevation $[I_b(0)/\sin\beta]$. The absorbed beam irradiance in sunflecks (I_{lbSun}), at the mean leaf angle, is given by the product of the beam intensity perpendicular to the beam and the mean cosine of the leaf angle and is independent of depth (Eqn A11). By definition, beam irradiance of shade leaves is zero. Total irradiance absorbed by sunlit leaves of each leaf angle class is the sum of absorbed beam plus absorbed diffuse irradiance (Eqn A12).

Solar geometry

Solar position was calculated from the geometry of planetary rotation. Solar elevation (β) is a function of day of the year (t_d), latitude (λ) and time of day (t) and is geometrically defined by the equations in Table A2. Solar noon was calculated from the longitude and the ephemeris of the sun. The latter was given by the equation of time, E_t (minutes), which accounts for the variation in the period of rotation of Earth (Iqbal 1983). The equation of time combined with the longitude correction determines the time (the number of hours after midnight) of solar noon. The longitude correction was based on 4 min for every degree difference between the local and standard meridians. All international standard meridians are multiples of 15° east or west of Greenwich, UK. For example, at Wagga Wagga (L_e = 147° 20·5' E and L_s = 150° E) the longitude correction was + 10·63 min and the correction E_t varied between –14·3 and + 16·4 min.

For the example given in the text on 25 October, $\delta = -23{\cdot}4(\pi/180)\cos[2\pi(298 + 10)/365] = -0{\cdot}23$ radians (Eqn A14) and E_t = 16·01 min (Eqn A17), so that, at Wagga Wagga, t_o = 11·91 h (11:55) (Eqn A16) and at 10:30, $h = \pi(10{\cdot}5 - 11{\cdot}91)/12 = -0{\cdot}37$ radians, so that at the latitude of Wagga Wagga (λ = –0·61 radians) $\sin\beta = -0{\cdot}57 \times -0{\cdot}23 + 0{\cdot}82 \times 0{\cdot}97 \times 0{\cdot}93 = 0{\cdot}87$ (Eqn A13).

Canopy reflection coefficients

In a canopy of uniform leaf angle distribution, the canopy reflection coefficient of beam irradiance, ρ_{cb}, is dependent on solar elevation, β, and is calculated empirically from the reflection coefficient of beam irradiance determined for a canopy with horizontal leaves and the beam extinction coefficient, $k_b = 0{\cdot}5/\sin\beta$ (Goudriaan 1977). The canopy reflection coefficient for diffuse irradiance was calculated by numerical integration of ρ_{cb} and the sky radiance over the hemisphere of the sky. Equations are presented in Table A2.

In the case of a uniform leaf angle distribution, with $\sigma = 0{\cdot}15$ (for PAR), $\rho_h = 0{\cdot}041$ (Eqn A20), so that with a uniform sky radiance the canopy reflection coefficient for diffuse irradiance is calculated as $\rho_{cd} = 0{\cdot}036$ (Eqn A21). In

Table A2. Equations to model incident radiation. Symbols are defined in Tables 2 and 3. *Note that Eqn A1b holds for longitudes measured east of Greenwich (cf. Iqbal 1983)

Equations	Definition	No.
Solar geometry		
$\sin\beta = \sin\lambda\sin\delta + \cos\lambda\cos\delta\cos h$	solar elevation angle	(A13)
$\delta = -23{\cdot}4\,\frac{\pi}{180}\cos[2\pi(t_d + 10)/365]$	solar declination angle	(A14)
$h = \pi(t - t_o)/12$	hour angle of sun	(A15)
$t_o = 12 + [4(L_s - L_e) - E_t]/60$	solar noon*	(A16)
$E_t = 0{\cdot}017 + 0{\cdot}4281\cos\Gamma_d - 7{\cdot}351\sin\Gamma_d - 3{\cdot}349\cos 2\Gamma_d - 9{\cdot}731\sin\Gamma_d$	equation of time	(A17)
$\Gamma_d = 2\pi(t_d - 1)/365$	day angle	(A18)
Canopy reflection coefficients		
$\rho_{cb}(\beta) = 1 - \exp[2\rho_h k_b/(1 + k_b)]$	beam irradiance, uniform leaf-angle distribution	(A19)
$\rho_h = \frac{1 - (1-\sigma)^{1/2}}{1 + (1-\sigma)^{1/2}}$	beam irradiance, horizontal leaves	(A20)
$\rho_{cd} = \frac{1}{I_d(0)}\int_0^{\frac{\pi}{2}} N_d(\alpha)\,\rho_{cb}(\alpha)\,d\alpha$	diffuse irradiance	(A21)

the example given in the main text, at 10:30 on 25 October $\rho_{cb} = 1 - \exp[-2\times0{\cdot}041 \times (0{\cdot}5/0{\cdot}87)/(1 + 0{\cdot}5/0{\cdot}87)] = 0{\cdot}029$.

Proportion of diffuse radiation

The proportion of diffuse radiation was calculated from a simple model of atmospheric attenuation of radiation under a cloudless sky (adapted from Campbell 1977),

$$I_b = a^m I_e \sin\beta, \tag{A22}$$

where I_b is beam PAR, I_e is the extra-terrestrial PAR quantum flux (2413 μmol m^{-2} s^{-1}, calculated from the energy distribution of the solar 'constant' – 1367 W m^{-2}; Iqbal 1983) and other symbols are defined in Table 3. The optical air mass, m, is defined as the ratio of the mass of atmosphere traversed per unit cross-sectional area of the solar beam to that traversed for a site at sea level if the sun was directly overhead and is calculated as

$$m = (P/P_o)/\sin\beta, \tag{A23}$$

where P is atmospheric pressure and P_o is atmospheric pressure at sea level.

The proportion of attenuated radiation that reaches the surface as diffuse radiation, f_a, has been observed to range from 40 to 45% under cloudless skies (Weiss & Norman 1985). A value of 42·6% was found to give a best fit to the data used in this paper (de Pury 1995). This can be expressed by the equation

$$I_d = f_a(1 - a^m) I_e \sin\beta, \tag{A24}$$

where I_d is diffuse radiation at the Earth's surface.

An expression for the fraction of diffuse radiation, f_d (proportion of total attenuated radiation, beam plus diffuse), for cloudless skies can be obtained by combining Eqns A22 and A24:

$$f_d = \frac{1 - a^m}{1 + a^m(1/f_a - 1)}. \tag{A25}$$

Although this model was originally developed for the attenuation of short-wave radiation, which has different scattering and absorption from PAR, we have assumed that the process is similar. These differences result in slightly different atmospheric transmission values based on PAR values compared to those based on short-wave radiation. For the example given in the main text $m = (98{\cdot}7/101{\cdot}3)/0{\cdot}87 = 1{\cdot}12$ so that $f_d = (1 - 0{\cdot}72^{1{\cdot}12}/[1 + 0{\cdot}72^{1{\cdot}12}(1/0{\cdot}426 - 1)] = 0{\cdot}159$.

APPENDIX 2: EQUATIONS FOR SHADED LEAVES

Absorbed irradiance

Irradiance absorbed by shaded leaves in a canopy is given as

$$\begin{aligned} I_{cSh} &= \int_0^{L_c} I_{lSh}(L)[1 - f_{Sun}(L)]dL \\ &= \int_0^{L_c} I_{ld}(L)[1 - f_{Sun}(L)]dL + \int_0^{L_c} I_{lbs}(L)[1 - f_{Sun}(L)]dL. \end{aligned} \tag{A26a}$$

The last line expresses the total irradiance absorbed by the shaded leaf area as the sum of diffuse and scattered diffuse irradiance absorbed by shaded leaves, from Eqns A5 and A1,

$$\begin{aligned} &\int_0^{L_c} I_{ld}(L)[1 - f_{Sun}(L)]dL = I_d(0)(1 - \rho_{cd}) \\ &\times \begin{bmatrix} 1 - \exp(-k'_d L_c) \\ -\{1 - \exp[-(k'_d + k_b)L_c]\}k'_d/(k'_d + k_b) \end{bmatrix}, \end{aligned} \tag{A26b}$$

and the scattered beam irradiance absorbed by shaded leaves, from Eqns A8 and A1,

$$\begin{aligned} &\int_0^{L_c} I_{lbs}(L)[1 - f_{Sun}(L)]dL = I_b(0) \\ &\times \begin{bmatrix} (1 - \rho_{cb})\begin{pmatrix} 1 - \exp(-k'_b L_c) \\ -\{1 - \exp[-(k'_b + k_b)L_c]\}k'_b/(k'_b + k_b) \end{pmatrix} \\ -(1 - \sigma)\{1 - \exp - (k_b L_c) - [1 - \exp(-2k_b L_c)]/2\} \end{bmatrix}. \end{aligned} \tag{A26c}$$

Photosynthetic capacity

Photosynthetic capacity of the shaded leaf fraction of the canopy, V_{cSh}, may be calculated by an integral of the leaf photosynthetic capacity (Eqn 12) and the shaded leaf area fraction (also from Eqn A1),

$$\begin{aligned} V_{cSh} &= \int_0^{L_c} V_l(L) f_{Sh}(L) dL \\ &= L_c \chi_n (N_o - N_b)\{[1 - \exp(-k_n)]/k_n \\ &\quad - [1 - \exp(-k_n - k_b L_c)]/(k_n + k_b L_c)\}. \end{aligned} \tag{A27}$$

ACKNOWLEDGEMENTS

This work was part of a PhD thesis written by D.deP. and supervised by G.D.F., S. C. Wong of ANU and O. T. Denmead of CSIRO, Centre for Environmental Mechanics. It was part of a larger project aimed to evaluate water-use efficiency of wheat in the field and involved many collaborators. Funding for D.deP. was provided by an ANU Post-Graduate Research Scholarship, a National Greenhouse Advisory Committee grant and a CSIRO-INRE scholarship. The project was initiated by a Rural Credits grant to G.D.F. We acknowledge valuable suggestions from an anonymous reviewer, and valuable discussions with Jon Lloyd.

REFERENCES

Acock B., Charles-Edwards D.A., Fitter D.J., Hand D.W., Ludwig L.J., Warren Wilson J. & Withers A.C. (1978) The contribution of leaves from different levels within a tomato crop to canopy net photosynthesis: an experimental examination of two canopy models. *Journal of Experimental Botany* **29**, 815–827.

Amthor J.S. (1994) Scaling CO_2-photosynthesis relationships from the leaf to the canopy. *Photosynthesis Research* **39**, 321–350.

Amthor J.S., Goulden M.L., Munger J.W. & Wofsy S.C. (1994) Testing a mechanistic model of forest-canopy mass and energy exchange using eddy correlation: carbon dioxide and ozone uptake by a mixed oak-maple stand. *Australian Journal of Plant Physiology* **21**, 623–651.

Anten N.P.R., Schieving F. & Werger M.J.A. (1995) Patterns of light and nitrogen distribution in relation to whole canopy carbon gain in C_3 and C_4 mono- and dicotyledonous species. *Oecologia* **101**, 504–513.

Badeck F.W. (1995) Intra-leaf gradient of assimilation rate and optimal allocation of canopy nitrogen: a model on the implications of the use of homogeneous assimilation functions. *Australian Journal of Plant Physiology* **22**, 425–439.

Badger M.R. & Collatz G.J. (1977) Studies on the kinetic mechanism of ribulose-1, 5-bisphosphate carboxylase and oxygenase reactions, with particular reference to the effect of temperature on kinetic parameters. *Carnegie Institute of Washington Yearbook* **76**, 355–361.

Baldocchi D.D. (1993) Scaling water vapor and carbon dioxide exchange from leaves to a canopy: rules and tools. In *Scaling Physiological Processes: Leaf to Globe* (eds J. R. Ehleringer & C. B. Field), pp. 77–114. Academic Press Inc., San Diego.

Björkman O., Badger M.R. & Armond P.A. (1980) Response and adaptation of photosynthesis to high temperatures. In *Adaptation of Plants to Water and High Temperature Stress* (eds N. C. Turner & P. J. Kramer), pp. 233–249. John Wiley & Sons. Inc., New York.

Boote K.J. & Loomis R.S. (1991) The prediction of canopy assimilation. In *Modeling Crop Photosynthesis – from Biochemistry to Canopy*, Special Publication no. 19 (eds K. J. Boote & R. S. Loomis), pp. 109–140. CSSA, Madison.

Caldwell M.M., Meister H.-P., Tenhunen J.D. & Lange O.L. (1986) Canopy structure, light microclimate and leaf gas exchange of *Quercus coccifera* L. in a Portuguese macchia: measurements in different canopy layers and simulations with a canopy model. *Trees* **1**, 25–41.

Campbell G.S. (1977) *An Introduction to Environmental Biophysics*. Springer-Verlag, New York.

Collatz G.J., Ball T.J., Grivet C. & Berry J.A. (1991) Physiological and environmental regulation of stomatal conductance, photosynthesis and transpiration: a model that includes a laminar boundary layer. *Agricultural and Forest Meteorology* **54**, 107–136.

Cowan I.R. (1968) The interception and absorption of radiation in plant stands. *Journal of Applied Ecology* **5**, 367–379.

de Pury D.G.G. (1995) *Scaling photosynthesis and water use from leaves to paddocks*. PhD thesis, The Australian National University, Canberra.

de Wit C.T. (1965) *Photosynthesis of Leaf Canopies*. Agricultural Research Report no. 663. PUDOC, Wageningen.

DeJong T.M. & Doyle J.F. (1985) Seasonal relationships between leaf nitrogen content (photosynthetic capacity) and leaf canopy irradiance exposure in peach (*Prunus persica*). *Plant, Cell and Environment* **8**, 701–706.

Duncan W.G., Loomis R.S., Williams W.A. & Hanau R. (1967) A model for simulating photosynthesis in plant communities. *Hilgardia* **38**, 181–205.

Evans J.R. (1983) Nitrogen and photosynthesis in the flag leaf of wheat (*Triticum aestivum* L.). *Plant Physiology* **72**, 297–302.

Evans J.R. & Farquhar G.D. (1991) Modelling canopy photosynthesis from the biochemistry of the C_3 chloroplast. In *Modelling Crop Photosynthesis – from Biochemistry to Canopy*, Special Publication no. 19 (eds K. J. Boote & R. S. Loomis), pp. 1–16. CSSA, Madison.

Farquhar G.D. (1989) Models of integrated photosynthesis of cells and leaves. *Philosophical Transactions of the Royal Society of London. Series B. Biological Sciences* **323**, 357–367.

Farquhar G.D., von Caemmerer S. & Berry J.A. (1980) A biochemical model of photosynthetic CO_2 assimilation in leaves of C_3 species. *Planta* **149**, 78–90.

Field C. (1983) Allocating leaf nitrogen for the maximization of carbon gain: leaf age as a control on the allocation program. *Oecologia* **56**, 341–347.

Field C. & Mooney H.A. (1986) The photosynthesis – nitrogen relationship in wild plants. In *On the Economy of Plant Form and Function* (ed. T. J. Givnish), pp. 25–55. Cambridge University Press, Cambridge.

Forseth I.N. & Norman J.M. (1993) Modelling of solar irradiance, leaf energy budget and canopy photosynthesis. In *Photosynthesis and Production in a Changing Environment: a Field and Laboratory Manual* (eds D. O. Hall, J. M. O. Scurlock, H. R. Bolhar-Nordenkampf, R. C. Leegood & S. P. Long), pp. 207–219. Chapman & Hall, London.

Goudriaan J. (1977) *Crop Micrometeorology: a Simulation Study*. PUDOC, Wageningen.

Goudriaan J. (1986) A simple and fast numerical method for the computation of daily totals of crop photosynthesis. *Agricultural and Forest Meteorology* **38**, 257–262.

Grant R.F. (1992) Interactions between carbon dioxide and water deficits affecting canopy photosynthesis: simulation and testing. *Crop Science* **32**, 1322–1328.

Hirose T. & Werger M.J.A. (1987) Maximising daily canopy photosynthesis with respect to the leaf nitrogen allocation pattern in the canopy. *Oecologia* **72**, 520–526.

Iqbal M. (1983) *An Introduction to Solar Radiation*. Academic Press, Toronto.

Johnson I.R., Parsons A.J. & Ludlow M.M. (1989) Modelling photosynthesis in monocultures and mixtures. *Australian Journal of Plant Physiology* **16**, 501–516.

Johnson I.R. & Thornley J.H.M. (1984) A model of instantaneous and daily canopy photosynthesis. *Journal of Theoretical Biology* **107**, 531–545.

Jones H.G. (1992) *Plants and Microclimate*. Cambridge University Press, Cambridge.

Jordan D.B. & Ogren W.L. (1984) The CO_2/O_2 specificity of ribulose, 1, 5-bisphosphate carboxylase/oxygenase. Dependence on ribulosebisphosphate concentration, pH and temperature. *Planta* **161**, 308–313.

Kirschbaum M.U.F. & Farquhar G.D. (1984) Temperature dependence of whole-leaf photosynthesis in *Eucalyptus pauciflora* Sieb. ex Spreng. *Australian Journal of Plant Physiology* **11**, 519–538.

Kriedemann P.E., Töröfalvy E. & Smart R.E. (1973) Natural occurrence and photosynthetic utilization of sunflecks by grapevine leaves. *Photosynthetica* **7**, 18–27.

Lemon E., Stewart D.W. & Shawcroft R.W. (1971) The sun's work in a cornfield. *Science* **164**, 371–378.

Lloyd J., Grace J., Miranda A.C., Meir P., Wong S.C., Miranda H.S., Wright I.R., Gash J.H.C. & McIntyre J. (1995) A simple calibrated model of Amazon rainforest productivity based on leaf biochemical properties. *Plant, Cell and Environment* **18**, 1129–1145.

Meister H.P., Caldwell M.M., Tenhunen J.D. & Lange O. (1987) Ecological implications of sun/shade-leaf differentiation in sclerophyllous canopies: assessment by canopy modeling. In *Plant Response to Stress* (eds J. D. Tenhunen *et al.)*, pp. 401–411. Springer-Verlag, Berlin.

Monsi M. & Saeki T. (1953) Über den lichtfaktor in den pflanzengesellschaften und seine bedeutung fur die stoffproduktion. *Japanese Journal of Botany* **14**, 22–52.

Norman J.M. (1979) Modeling the complete crop canopy. In *Modification of the Aerial Environment of Plants* (eds B. J. Barfield & J. F. Gerber), pp. 249–277. American Society Agricultural Engineers, St. Joseph, Michigan.

Norman J.M. (1980) Interfacing leaf and canopy irradiance interception models. In *Predicting Photosynthesis for Ecosystem Models*, Vol. II (eds J. D. Hesketh & J. W. Jones), pp. 49–67. CRC Press, Inc., Boca Raton, FL.

Norman J.M. (1982) Simulation of microclimates. In *Biometeorology in Integrated Pest Management* (eds J. L. Hatfield & I. J. Thomason), pp. 65–99. Academic Press, New York.

Norman J.M. (1993) Scaling processes between leaf and canopy levels. In *Scaling Physiological Processes: Leaf to Globe* (eds J. R. Ehleringer & C. B. Field), pp. 41–76. Academic Press, Inc., San Diego.

Norman J.M. & Polley W. (1989) Canopy photosynthesis. In *Photosynthesis*, Vol. 8 (ed. W. R. Briggs), pp. 227–241. Alan R. Liss, Inc., New York.

Pons T.L., Schieving F., Hirose T. & Werger M.J.A. (1989) Optimization of leaf nitrogen allocation for canopy photosynthesis in *Lysimachia vulgaris*. In *Causes and Consequences of Variation in Growth Rate and Productivity of Higher Plants* (eds H. Lambers, M. L. Cambridge, H. Konings & T. L. Pons), pp. 175–186. SPB Academic Publishing BV, The Hague.

Raupach M.R. (1995) Vegetation–atmosphere interaction and surface conductance at leaf, canopy and regional scales. *Agricultural and Forest Meteorology* **73**, 151–179.

Reynolds J.F., Chen J.L., Harley P.C., Hilbert D.W., Dougherty R.L. & Tenhunen J.D. (1992) Modeling the effects of elevated CO_2 on plants: extrapolating leaf response to a canopy. *Agricultural and Forest Meteorology* **61**, 69–94.

Ross J. (1975) Radiative transfer in plant communities. In *Vegetation and the Atmosphere*, Vol. 1, *Principles* (ed. J. L. Monteith), pp. 13–55. Academic Press, London.

Ross J. (1981) *The Radiation Regime and Architecture of Plant Stands*. Dr W.Junk Publishers, The Hague.

Ross J. & Nilson T. (1967) The spatial orientation of leaves in crop stands and its determination. In *Photosynthesis of Productive Systems* (ed. A. A. Nichiporovich), pp. 86–99. Academy of Sciences of the USSR, Jerusalem.

Sadras V.O., Hall A.J. & Connor D.J. (1993) Light-associated nitrogen distribution profile in flowering canopies of sunflower (*Helianthus annuus* L.) altered during grain growth. *Oecologia* **95**, 488–494.

Sands P.J. (1995) Modelling canopy production. I. Optimal distribution of photosynthetic resources. *Australian Journal of Plant Physiology* **22**, 593–601.

Sayed O.H., Earnshaw M.J. & Emes M.J. (1989) Photosynthetic responses of different varieties of wheat to high temperature. II. Effect of heat stress on photosynthetic electron transport. *Journal of Experimental Botany* **40**, 633–638.

Schieving F., Pons T.L., Werger M.J.A. & Hirose T. (1992) The vertical distribution of nitrogen and photosynthetic activity at different plant densities in *Carex acutiformis*. *Plant and Soil* **14**, 9–17.

Sellers P.J., Berry J.A., Collatz G.J., Field C.B. & Hall F.G. (1992) Canopy reflectance, photosynthesis, and transpiration. III. A reanalysis using improved leaf models and a new canopy integration scheme. *Remote Sensing of Environment* **42**, 187–216.

Sinclair T.R., Murphy C.E. & Knoerr K.R. (1976) Development and evaluation of simplified models for simulating canopy photosynthesis and transpiration. *Journal of Applied Ecology* **13**, 813–829.

Smolander H. (1984) Measurement of fluctuating irradiance in field studies of photosynthesis. *Acta Forestalia Fennica* **187**, 1–56.

Spiertz J.H.J. & Ellen J. (1978) Effects of nitrogen on crop development and grain growth of winter wheat in relation to assimilation and utilization of assimilates and nutrients. *Netherlands Journal of Agricultural Science* **26**, 210–231.

Terashima I. & Hikosaka K. (1995) Comparative ecophysiology of leaf and canopy photosynthesis. *Plant, Cell and Environment* **18**, 1111–1128.

von Caemmerer S., Evans J.R., Hudson G.S. & Andrews T.J. (1994) The kinetics of ribulose-1, 5-bisphosphate carboxylase/oxygenase *in vivo* inferred from measurements of photosynthesis in leaves of transgenic tobacco. *Planta* **195**, 88–97.

Wang Y.P. & Jarvis P.G. (1993) Influence of shoot structure on the photosynthesis of Sitka spruce (*Picea sitchensis*). *Functional Ecology* **7**, 433–451.

Warren Wilson J. (1960) Inclined point quadrats. *New Phytologist* **59**, 1–8.

Watanabe N., Evans J.R. & Chow W.S. (1994) Changes in the photosynthetic properties of Australian wheat cultivars over the last century. *Australian Journal of Plant Physiology* **21**, 169–183.

Weiss A. & Norman J.M. (1985) Partitioning solar radiation into direct and diffuse, visible and near-infrared components. *Agricultural and Forest Meteorology* **34**, 205–213.

Whisler F.D., Acock B., Baker D.N., Fye R.E., Hodges H.F., Lambert J.R., Lemmon H.E., McKinion J.M. & Reddy V.R. (1986) Crop simulation models in agronomic systems. *Advances in Agronomy* **40**, 141–208.

Wu R.L. (1993) Simulated optimal structure of a photosynthetic system: implication for the breeding of forest crop ideotype. *Canadian Journal Forest Research* **23**, 1631–1638.

Wullschleger S.D. (1993) Biochemical limitations to carbon assimilation in C_3 plants – A retrospective analysis of the A/C_i curves from 109 species. *Journal of Experimental Botany* **44**, 907–920.

Received 18 June 1996; received in revised form 10 December 1996; accepted for publication 10 December 1996